DOI: http://dx.doi.org/10.2138/am-2018-6166

# Revision 1

INVITED CENTENNIAL ARTICLE

# Secular change in metamorphism and the onset of global plate tectonics

MICHAEL BROWN[1,]* AND TIM JOHNSON[2]

[1]Laboratory for Crustal Petrology, Department of Geology, University of Maryland, College Park, MD 20742, U.S.A.
[2]Department of Applied Geology, The Institute for Geoscience Research (TIGeR), Curtin University, Perth WA 6845, Australia

________________

* Email: mbrown@umd.edu

## ABSTRACT

On the contemporary Earth, distinct plate tectonic settings are characterized by differences in heat flow that are recorded in metamorphic rocks as differences in apparent thermal gradients. In this study we compile thermal gradients (defined as temperature (*T*)/pressure (*P*) at the metamorphic peak) and ages of metamorphism (defined as the timing of the metamorphic peak) for 456 localities from the Eoarchean to Cenozoic Eras to test the null hypothesis that thermal gradients of metamorphism through time did not vary outside of the range expected for each of these distinct plate tectonic settings. Based on thermal gradients, metamorphic rocks are classified into three natural groups: high d*T*/d*P* (>775 °C/GPa, mean ~1110 °C/GPa (n = 199)rates), intermediate d*T*/d*P* (775–375 °C/GPa, mean ~575 °C/GPa (n = 127)) and low d*T*/d*P* (<375 °C/GPa, mean ~255 °C/GPa (n = 130)) metamorphism. Plots of *T*, *P* and *T*/*P* against age demonstrate the widespread occurrence of two contrasting types of metamorphism—high d*T*/d*P* and intermediate d*T*/d*P*—in the rock record by the Neoarchean, the

widespread occurrence of low d*T*/d*P* metamorphism in the rock record by the end of the Neoproterozoic, and a maximum in the thermal gradients for high d*T*/d*P* metamorphism during the period 2.3 to 0.85 Ga. These observations falsify the null hypothesis and support the alternative hypothesis that changes in thermal gradients evident in the metamorphic rock record were related to changes in geodynamic regime. Based on the observed secular changes, we postulate that the Earth has evolved through three geodynamic cycles since the Mesoarchean and has just entered a fourth. Cycle I began with the widespread appearance of paired metamorphism in the rock record, which was coeval with the amalgamation of widely dispersed blocks of protocontinental lithosphere into supercratons, and was terminated by the progressive fragmentation of the supercratons into protocontinents during the Siderian–Rhyacian (2.5 to 2.05 Ga). Cycle II commenced with the progressive reamalgamation of these protocontinents into the supercontinent Columbia and extended until the breakup of the supercontinent Rodinia in the Tonian (1.0 to 0.72 Ga). Thermal gradients of high d*T*/d*P* metamorphism rose around 2.3 Ga leading to a thermal maximum in the mid-Mesoproterozoic, reflecting insulation of the mantle beneath the quasi-integral continental lithosphere of Columbia, prior to the geographical reorganization of Columbia into Rodinia. This cycle coincides with the age span of most anorogenic magmatism on Earth and a scarcity of passive margins in the geological record. Intriguingly, the volume of preserved continental crust of Mesoproterozoic age is low relative to the Paleoproterozoic and Neoproterozoic Eras. These features are consistent with a relatively stable association of continental lithosphere between the assembly of Columbia and the breakup of Rodinia. The transition to Cycle III during the Tonian is marked by a steep decline in the thermal gradients of high d*T*/d*P* metamorphism to their lowest value and the appearance of low d*T*/d*P* metamorphism in the rock record. Again, thermal gradients for high d*T*/d*P* metamorphism

show a rise to a peak at the end of the Variscides during the formation of Pangea, before another steep decline associated with the breakup of Pangea and the start of a fourth cycle at ca 0.175 Ga. Although the mechanism by which subduction started and plate boundaries evolved remains uncertain, based on the widespread record of paired metamorphism in the Neoarchean we posit that plate tectonics was established globally during the late Mesoarchean. During the Neoproterozoic there was a change to deep subduction and colder thermal gradients, features characteristic of the modern plate tectonic regime.

**Keywords:** *P–T–age* of metamorphism, thermal gradients, subduction, geodynamic cycles, blueschist, eclogite, Invited Centennial article

## INTRODUCTION

Regional metamorphism during the Cenozoic Era is linked to plate tectonics. It occurs at: divergent plate boundaries, where newly generated oceanic crust is metamorphosed following hydrothermal circulation of sea water; convergent plate boundaries, where subduction, or subduction followed by collision, pulls crustal rocks deep into the mantle during orogenesis, and where orogenic plateaus may be developed in the hinterland; and, at plate boundaries that involve mainly lateral displacements (Brown 2006). Of particular importance to humanity are metamorphic processes at both contemporary and ancient convergent plate boundaries, because they are responsible for a majority of contemporary earthquakes and they generated our ancient mineral endowments (Stern 2002).

At contemporary convergent plate boundaries, intermediate (50–300 km) and deep (300–670 km) focus earthquakes are concentrated in subduction zones, and are dominantly caused by metamorphic reactions. Intermediate-depth earthquakes most likely are triggered by metamorphic devolatilization reactions in either the crust (during cold subduction) or the upper serpentinized part of the underlying mantle (during warm subduction) that together comprise the downgoing lithosphere (Hacker 2003; Rondenay et al. 2008; van Keken et al. 2012; Abers et al. 2013; Okazaki and Hirth 2016), although the interplay between thermal and mechanical feedbacks (John et al. 2009; Ohuchi et al. 2017) and reaction-induced grain size reduction (Incel et al. 2017) have been proposed as alternative mechanisms. Deep earthquakes occur in the interior of the subducting lithosphere slab and are most likely triggered by the metastable transformation of olivine to spinel (Green and Burnley, 1989; Kirby et al., 1991, 1996). By contrast, earthquakes in collisional belts are related to the strong lower crust of the orogenic hinterland that is thought to be essentially anhydrous due to one or more episodes of high-grade metamorphism and melt loss to the upper crust (Maggi et al. 2000; Jackson et al. 2008; Sloan et al., 2011). Ancient convergent plate boundaries are important to society because the formation of metallogenic ore deposits, which underpin both technological advances and economic development, is associated with fluid flow in these tectonic settings (McCuaig and Kerrich 1998; Goldfarb et al. 2010; Tomkins 2010; Cawood and Hawkesworth 2015; Zhong et al. 2015).

## Contemporary metamorphism

Clasts of metamorphosed mafic rock with incipient blueschist facies mineral assemblages associated with serpentinized peridotites have been recovered during drilling into a seamount in the Mariana forearc. These incipient blueschists comprise aragonite, sodic pyroxene, lawsonite, albite and quartz, which indicate pressure–temperature ($P$–$T$) conditions of ~0.6 GPa and ~200 °C (Maekawa et al., 1993). Similarly, transitional blueschist–greenschist facies rocks occur in the non-volcanic outer Banda Arc of Eastern Indonesia, in which overprinting mineral assemblages suggest decompression from $P$ of ~0.7 to ~0.4 GPa at $T$ between 300 and 400 °C (Kadarusman et al. 2010). These rocks record $P$–$T$ conditions that are consistent with thermal models for the shallow parts of active subduction zones (Syracuse et al. 2010). Thus, in a plate tectonic regime, we relate blueschist metamorphism to subduction.

By contrast, high-grade metamorphism occurs in a variety of plate tectonic settings. For example, mafic granulites have been scavenged from the deeper parts of thick Mesozoic oceanic plateaus (Gregoire et al., 1994) and occur in exposed middle-to-lower crust of young continental arcs (Lucassen and Franz, 1996). Similarly, metapelitic xenoliths retrieved from Neogene volcanoes in central Mexico (Hayob et al., 1989) and at El Joyazo in south-eastern Spain (Cesare and Gomez-Pugnaire, 2001; Ferri et al. 2007) have been argued to record evidence of Cenozoic to present day high-temperature metamorphism in the lower crust. Also, evidence of melt-related processes in garnet granulite xenoliths from Kilbourne Hole, Rio Grande Rift, suggests contemporary high-temperature metamorphism in the lower crust of rifts (Scherer et al., 1997).

Recent continental backarcs are hot with uniformly thin and weak lithosphere over considerable areas (Hyndman 2015; Hyndman et al., 2005). They represent an inevitable locus of deformation leading to thickening, producing an environment suitable for high-grade metamorphism. In addition, collisional orogenesis is important because both initial orogenic thickening and later orogenic collapse disrupt the steady-state thermal structure of the lithosphere (Clark et al. 2011; Dewey 1988). These processes are consistent with the inference from multiple geophysical datasets of mica breakdown melting in the deep crust of the Altiplano and Tibet (Schilling and Partzsch 2001; Li et al. 2003).

## SECULAR CHANGE IN METAMORPHISM: HISTORICAL PERSPECTIVE

De Roever first raised the issue of secular change in metamorphism in his landmark paper "Some differences between post-Paleozoic and older regional metamorphism" (de Roever 1956; see also de Roever 1965). He argued that the preferential occurrence of rocks with mineral assemblages characteristic of the glaucophane schist facies (*sic*) in Mesozoic and Cenozoic orogenic belts, combined with the observation that known occurrences of lawsonite were restricted to the same period, suggested lower thermal gradients after the Paleozoic. Pushing back the transition, Ernst (1972) discussed the occurrence and mineralogic evolution of blueschist belts with time, noting their virtual absence from the Precambrian. In a plate tectonics context, he argued for a temporal decrease in geothermal gradient and thickening of the lithosphere during the Phanerozoic.

With regard to secular change during the Precambrian, Grambling (1975) argued that metamorphic geotherms had declined while average metamorphic pressures had increased with time. In a novel semi-quantitative approach, Grambling derived his *P*–*T* estimates by comparing 100 published mineral assemblages to a model petrogenetic grid he constructed from available experimental data, thus ensuring internal consistency between relative values even if the absolute values were not accurate. By contrast, in an early example using experimentally calibrated barometers, Perkins and Newton (1981) argued that the cluster of pressures at 0.85 ± 0.2 GPa for nine Precambrian granulite terrains suggested a common repeated petrogenesis, and further that crustal thicknesses in the late Archean were similar to those of present-day stable crust.

It is instructive to remember that thirty years ago quantitative thermobarometry was in its infancy, comprehensive internally consistent themodynamic datasets were only just being developed and fully quantitative *P*–*T* phase diagrams for large chemical systems approaching the complexity of natural rocks still lay in the future. Indeed, it was another twenty years before a sufficient number of reliable *P–T* and age data were available to allow an analysis of secular change based on metamorphic mineral assemblages (Brown 2007).

During the same period, following the discovery that large areas of lower crustal rocks exposed in Antarctica record peak temperatures >1000 °C (Ellis et al., 1980), more than fifty localities globally have been shown to record peak temperatures >900 °C (Kelsey and Hand 2014), the arbitrary lower temperature chosen to separate ultrahigh-temperature (UHT) granulites from common granulites (Harley 1998). In spite of the number of UHT localities, no more than a few record confirmed temperatures >1000°C (Harley 2008; Kelsey and Hand 2014; Korhonen et al. 2014). Only a few years later, the exciting realm of ultrahigh-pressure (UHP) metamorphism was uncovered through the identification of coesite in pyrope–quartz schists of the Dora Maira massif in the Western Alps (Chopin, 1984) and confirmation of its occurrence in eclogite from Norway (Smith, 1984). Rocks with spectacular mineral assemblages and incomplete reaction microstructures formed during exhumation and/or cooling are characteristic of both types of extreme metamorphism (Chopin 2003; Harley 2008; Kelsey and Hand 2014).

More surprising still has been the discovery of microdiamonds in several UHP metamorphic terranes (Dobrzhinetskaya 2012), the extreme pressures of ~7 GPa apparently recorded in the Sulu belt (Ye et al. 2000) and in the Kokchetav massif (Katayama and Maruyama, 2009), and the evidence of former stishovite in deeply subducted metasedimentary rocks (Liu et al. 2007). Although outside of our scope in this article, it is worth noting that the stimulus provided by the growth of interest in UHP metamorphism combined with rapid advances in microanalytical techniques has opened up a new era in our understanding of how deep subduction recycles crustal materials through the mantle (Liou et al. 2014; Griffin et al. 2016).

## METAMORPHISM AND PLATE TECTONICS

The relationship between metamorphism and plate tectonics has evolved since the introduction of the "New global tectonics" in 1968 (Isacks et al. 1968). Ernst (1971, 1973) was quick to recognize the relationship between low d*T*/d*P* metamorphism, particularly blueschist metamorphism, and subduction. More recent contributions include those by Maruyama and Liou concerning blueschists (Liou et al. 1990; Maruyama et al. 1996; Maruyama and Liou 1998, 2005), Godard (2001) concerning eclogites, Chopin (2003) concerning UHP metamorphic rocks, and Tsujimori et al. (2006) and Tsujimori and Ernst (2014) concerning lawsonite-bearing blueschists and eclogites. Stern (2005) and Brown (2006, 2007, 2014) addressed the issue of secular change and the onset of plate tectonics.

An important feature of Earth's plate tectonic regime is that ocean lithosphere dips under an arc at convergent plate boundaries. In this regime, the downgoing slab depresses isotherms creating an environment with low d*T*/d*P*, whereas fluids and melts generated by breakdown of hydrous minerals in the crust and serpentinized upper mantle layer of the downgoing slab promote magma generation in the mantle wedge above, leading to advective high d*T*/d*P* in the overriding plate (Oxburgh and Turcotte, 1970). This is the tectonic setting in which paired metamorphic belts develop, as envisaged by Miyashiro (1961, 1973) and modeled by Oxburgh and Turcotte (1971). The ocean-side belt is the site of lower d*T*/d*P* metamorphism whereas the hinterland-side belt is the site of higher d*T*/d*P* metamorphism. Subsequently, in a series of articles, Brown (1998a, 1998b, 2002, 2010) has argued that although paired metamorphic belts

This is a preprint, the final version is subject to change, of the American Mineralogist (MSA)
Cite as Authors (Year) Title. American Mineralogist, in press.
DOI: http://dx.doi.org/10.2138/am-2018-6166

may be contemporaneous they need not necessarily have been spatially adjacent during formation, but more commonly were juxtaposed subsequently during strike slip translation along the trench.

Since the late Tonian, the ocean-side belt of a paired system has been characterized by low $\mathrm{d}T/\mathrm{d}P$ metamorphism generating blueschists and low temperature eclogites, and coesite and diamond facies UHP metamorphic rocks (Brown 2009). The hinterland-side belt is of high $\mathrm{d}T/\mathrm{d}P$ type and is generally characterized by high $\mathrm{d}T/\mathrm{d}P$ metamorphism that may reach granulite facies or even UHT metamorphic conditions in backarcs. If subduction is terminated, then backarcs with thin lithosphere may generate counter-clockwise $P$–$T$ paths due to thickening and thermal decay as they cool (Oxburgh 1990).

Horizontal plate motions lead to collisions between arcs, ribbon terranes, ocean plateaus and continents preserving evidence of low $\mathrm{d}T/\mathrm{d}P$ metamorphism in the suture (Brown 2009). These plate collisions also create thickened lithosphere to generate intermediate $\mathrm{d}T/\mathrm{d}P$ metamorphism in the mountain belt, commonly marked by high-pressure granulites and medium- or high-temperature eclogites, and high $\mathrm{d}T/\mathrm{d}P$ metamorphism in the orogenic hinterland, which generates granulites associated with mountain plateaus. If crust is enriched in heat producing elements, then the generally low erosion rates of mountain plateaus generates UHT metamorphic rocks with clockwise $P$–$T$ paths (Clark et al. 2011).

Plate tectonics has provided us with a context to understand contemporary metamorphism and its relationship to different tectonic settings, and has allowed us to extend this relationship at least as far back as the dawn of the Phanerozoic (Stern 2005; Brown 2006). However, during the Precambrian the ambient upper mantle temperature is thought to have been higher than the present day and consequently geodynamics may have been different (Davis 2006; van Hunen and van den Berg 2008; Sizova et al. 2010, 2014, 2015; Herzberg 2016). Indeed, a strong case has been made for a stagnant-lid plate tectonic regime associated with plume tectonics on the early Earth (Fischer and Gerya 2016; Griffin et al. 2013; Gerya 2014; Johnson et al. 2014, 2017; O'Neill and Debaille 2014; Sizova et al. 2015).

## SECULAR CHANGE IN MANTLE TEMPERATURE

The thermal history of the Earth is poorly constrained (Korenaga 2013; Labrosse and Jaupart 2007; Silver and Behn 2008; van Hunen and Moyen 2012). Petrological data indicate that ambient mantle potential temperatures were higher in the Archean—although how much higher than the present day is uncertain, perhaps 150–250 °C—with a similar range of global variations (Herzberg et al. 2007, 2010; Condie et al. 2016; Herzberg 2016; Putirka 2016; Ganne and Feng 2017). Furthermore, the mantle potential temperature at the end of crystallization of the magma ocean and whether the mantle was warming during the Eoarchean–Mesoarchean to a high in the Mesoarchean–Neoarchean are open questions. Thermal history calculations (Labrosse and Jaupart 2007) yield a maximum $\Delta T$ from the present day ambient mantle potential temperature of ~250 °C at 3.0 Ga. Although these calculations cannot be extrapolated further back in time, Labrosse and Jaupart (2007) argue that the mantle was ~200 °C hotter than the present day at the start of mantle convection after crystallization of the last magma ocean. Thus, it is likely that prior to ca 3.0 Ga heating from radioactive decay exceeded surface heat loss, whereas since that time secular cooling has dominated the thermal history of the Earth (Labrosse and Jaupart 2007; Korenaga 2008; Ganne and Feng 2017).

The rheology of the lithosphere and underlying mantle are strongly dependent on temperature, which in turn affects the geodynamics (Sizova et al. 2010, 2014). Thus, a hotter and warming upper mantle may have prevented subduction in the Hadean–Archean forcing Earth to operate in a different geodynamic regime from that today (Johnson et al. 2014, 2017; O'Neill and Debaille 2014; Sizova et al. 2015; Fischer and Gerya 2016). If correct, models based on uniformitarian principles may be misleading. Furthermore, Jaupart et al. (2016) have argued that at the time of crustal stabilization, Moho temperatures were near solidus values. Such conditions would have favored lithosphere foundering by Rayleigh–Taylor instabilities (Jull and Kelemen 2001; Toussaint et al. 2004), which may have played a much more important role in lithosphere evolution on the early Earth than on contemporary Earth (Johnson et al. 2014; O'Neill and Debaille 2014; Sizova et al. 2015; Fischer and Gerya 2016).

## OBJECTIVE OF THIS STUDY

At issue is whether a hotter mantle and higher heat production in the past precluded subduction, the linking of mobile belts sensu Wilson (1965) and the operation of global plate tectonics. A characteristic feature of contemporary subduction is that it is one-sided (Gerya et al. 2008), leading to the development of two contrasting thermal environments at convergent plate boundaries (Oxburgh and Turcotte, 1970, 1971), one representing the subduction zone or collisional suture (cooler) and the other forming the arc–backarc system or orogenic hinterland (warmer). If plate tectonics did not operate from early in the Hadean, or if plate tectonics operated in the Hadean but switched off as the mantle heated during the early Archean, then to identify the onset of plate tectonics we must recognize the first imprint of one-sided subduction in the rock record, and we must decide if that imprint is one of only a few, reflecting local processes, or one of many, reflecting global behavior. Brown (2006) showed that different types of metamorphism would be registered in each of these thermal environments, producing paired metamorphic belts (Miyashiro 1961; Brown 2010), and proposed that the record of metamorphism in ancient orogens may be inverted to determine when this style of subduction was first registered in the geological record (Brown 2008, 2014).

Using a new dataset of 456 robust determinations of peak metamorphic *P–T* conditions and ages retrieved from the rock record back to the Eoarchean, we address the question: Can we recognize a duality of metamorphic types back through the whole geological record and, if not, can we identify the onset of global plate tectonics based on evidence from the metamorphic rock record? One challenge to consider in reading the rock record is preservation bias. In addition, we must weigh global (commonly younger) vs local (commonly older) datasets and attempt to distinguish initiation from episodic or continuous (local or global) subduction.

## METHODS AND CAVEATS

### Methods

To extend the relationship between metamorphism and tectonic setting back into the Precambrian and address the question of when plate tectonics may be first recognized in the geological record, we use the 'forensic' methods developed by metamorphic petrologists to read the history of individual rock samples. This approach allows us to decode the mineralogical and microstructural evidence of burial/heating and exhumation/cooling imprinted on pre-existing sedimentary, igneous and metamorphic rocks by processes such as subduction, accretion, trench advance or retreat, delamination, collisional orogenesis and orogenic collapse (Brown 2008, 2009). This study is based on an extensive review of literature data up to mid-2016, with minor corrections/additions in 2017. We have restricted our dataset to crustal protoliths, insofar as the protoliths can be identified with confidence. Thus, we do not include data from orogenic peridotites. We did not include the regional contact metamorphism of the classic Buchan block in northeast Scotland, which is characterized by granulite facies temperatures at very low pressures reflecting the unusual and extreme thermal gradients produced by advective heat (Johnson et al. 2015). Also, we have excluded newly recognized occurrences of ultrahigh-pressure minerals in chromitites associated with ophiolitic complexes and in mantle xenoliths; these occurrences, which record recycling of crustal materials by deep subduction and subsequent mantle upwelling rather than orogenesis, were recently reviewed by Liou et al. (2014). The principal outputs that we use are quantitative estimates of pressure ($P$) and temperature ($T$), from which we derive an apparent thermal gradient ($T/P$), and geochronology to provide the age ($t$) of each $P$–$T$ datum. Our task in this study is to invert these data to interpret geodynamics.

**The dynamic nature of regional metamorphism.** Burial and heating and exhumation and cooling yield clockwise (in $P$–$T$ space) $P$–$T$–$t$ paths that reflect an evolution crossing from lower to higher thermal gradients with time. By contrast, heating and burial and cooling and exhumation yield counter-clockwise $P$–$T$–$t$ paths that reflect an evolution crossing from higher to lower thermal gradients with time. Evolution of pressure and temperature with time leads to changes in modes and compositions of phases; mode and composition, and 'age' become fixed at some point along the $P$–$T$–$t$ path, but not necessarily at the same point. The maximum pressure ($P_{max}$) and temperature ($T_{max}$) generally do not coincide; along clockwise $P$–$T$–$t$ paths, $P_{max}$ commonly occurs before $T_{max}$, whereas along counter-clockwise $P$–$T$–$t$ paths, $T_{max}$ commonly occurs before $P_{max}$. In the absence of a prograde record, many published $P$–$T$ data are inferred to represent 'peak' $P$–$T$ conditions, but some represent $P_{max}$ or $T_{max}$ conditions. Similarly, many published ages are inferred to record the timing of 'peak' *P–T* conditions, but some may record late prograde and some retrograde *P–T* conditions. For these reasons we have carefully reviewed *P–T* and age data from the literature and compiled our own best estimate of peak *P–T* and *t* for each location in the dataset. The references in the Supplementary Data Table are only those necessary to support the data summarized therein rather than a full bibliography for each location.

**Pressure and temperature.** For each location, we quote a single *P–T* value, which records a single apparent thermal gradient crossed during a dynamic evolution from lower to higher or higher to lower gradients. The *P–T* value may be based on multiple samples and/or multiple thermobarometric methods and/or multiple published studies. We have used as much recent data as possible, oriented towards phase diagram (pseudosection) thermobarometry rather than conventional thermobarometry, for the reasons given by Powell and Holland (2008), particularly for high temperature metamorphism where conventional thermometry may be unreliable. Many classic localities have a long history of study, and in these circumstances we have tried to use the most appropriate recent quantitative data.

**Age.** The *P–T* conditions must be linked to an age of metamorphism, which may be determined by various methods using both rock-forming and accessory minerals, as recently reviewed by Kohn (2016) in his Centennial article. Of particular importance in metamorphic studies has been the development of rapid *in situ* analysis, first using secondary ionization mass spectrometry, and then laser ablation inductively coupled plasma mass spectrometry and most recently laser ablation split-stream (LASS) inductively coupled plasma mass spectrometry. The advantage of LASS is that it permits rapid simultaneous analysis of isotope and elemental compositions of accessory minerals (Kylander-Clark et al. 2013). This allows us to take advantage of our better understanding of the partitioning of trace elements between rock-forming and accessory minerals to potentially link ages with *P–T* conditions (Rubatto and Hermann 2008; Taylor et al. 2015, 2017).

Although a variety of different methods are in use today, U–Pb chronology on zircon and monazite is commonly preferred. However, U–Pb chronology on titanite and rutile, Lu–Hf and Sm–Nd chronology on garnet, Rb–Sr chronology on micas, and $^{40}Ar/^{39}Ar$ chronology on amphiboles and micas are also used in appropriate circumstances. The principal methods by which we link metamorphic *P–T* conditions and ages (*t*) include textural and/or chemical correlation, particularly inclusion relationships and the inferred presence or absence of garnet in equilibrium with zircon (Rubatto and Hermann 2008; Taylor et al. 2015, 2017), and combined chronologic and thermometric microanalysis, such as simultaneous *T–t* determinations on zircon, titanite and rutile (Kohn 2016; Taylor et al. 2016). However, caution is still required when dealing with rocks that formed at suprasolidus or at ultrahigh pressure conditions (Yakymchuk and Brown 2014; Kohn et al. 2015), or that were deformed and retrogressed during exhumation (Reddy et al. 1997).

**Caveats**

This analysis relies on several important issues relating to the record of metamorphism in the geological record.

**Equilibrium.** The principal requirement is that the close-to-peak mineral assemblages are robust recorders of *P* and *T*. Substantial *a posteriori* evidence indicates that mineral assemblages in rocks undergoing prograde metamorphism equilibrate continuously on some scale as fluid or melt is being generated, but undergo little or no change during the retrograde evolution once the subsolidus rock becomes fluid absent (around peak *T*) or following final crystallization of melt on cooling to the solidus (Powell et al. 2005). This principal is supported by the metamorphic facies concept, which has demonstrated repeated occurrences of the same mineral assemblages in rocks of equivalent chemical composition at similar metamorphic grades throughout the geological record.

Thus, an equilibrium mineral assemblage that records the *P*–*T* conditions of final fluid loss or crossing of the solidus is likely to be preserved during exhumation and cooling, because these mineral assemblages are commonly anhydrous and are difficult to retrogress or overprint without fluid influx. For this reason, our study has been limited to rocks equilibrated under conditions of relatively high temperature and/or pressure. For medium- and high-temperature metamorphism at $P < 1$ GPa, we set a minimum temperature for inclusion at approximately 600 °C (with three exceptions), whereas for higher pressure metamorphism at $T < 600$ °C, we applied a minimum pressure of approximately 1 GPa to ensure a reasonable temperature of metamorphism and the likelihood of an equilibrated peak mineral assemblage (with one exception). Using these thresholds, the resulting *P*–*T* data are believed to be robust.

**Tectonic overpressure.** The relationship between the mechanical pressure (the mean stress) and the thermodynamic pressure (the value we calculate from the mineral assemblage) is an underappreciated issue that has recently come to the fore in metamorphic petrology (Hobbs and Ord 2017). For practical purposes, the thermodynamic pressure may be taken as close to the mean stress (Hobbs and Ord 2016), but the common assumption that thermodynamic pressure is equal to the lithostatic load is false, although in weak homogeneous lithosphere the differences between lithostatic load, mean stress and thermodynamic pressure may be small. The difference between the mean stress and the pressure arising from the lithostatic load is referred to as tectonic pressure or overpressure (Mancktelow 1995, 2005). Assessing the possible influence of tectonic overpressure on metamorphic phase equilibrium is a matter of current debate (Wheeler, 2014; Dabrowski et al. 2015; Tajcmanová et al. 2015; Hobbs and Ord 2017).

The common interpretation that UHP metamorphic rocks have been exhumed from mantle depths is based on the assumption that calculated pressure approximates lithostatic load and may be converted to depth. However, if the calculated pressure was larger than lithostatic due to tectonic overpressure, for example when the flow is confined (Mancktelow 1995, 2005), then metamorphic rocks were formed at shallower depths than expected based on any simplistic pressure-to-depth conversion. Recent thermomechanical numerical simulations of subduction-to-collision orogenesis suggest that pressures may reach twice the lithostatic load on million year timescales in dry and strong heterogeneous continental crust during subduction (Gerya 2015; Reuber et al. 2016). This result indicates that there could be significant differences in the magnitude of tectonic overpressure between different types of metamorphic terrane (e.g. low *T/P* vs high *T/P*), since the rheology of rocks has an exponential dependence on temperature (Turcotte and Schubert 2002). Nonetheless, we expect that tectonic processes and thermal gradients associated with any one type of metamorphic terrane may be similar whether or not there is a component of tectonic overpressure. This inference is confirmed by the success of the metamorphic facies concept. Thus, we believe tectonic overpressure is not a problem in this study, which uses calculated (thermodynamic) pressures. It follows that we should quote thermal gradients in terms of *T*/*P*, not *T*/depth as is common practice.

**Retrogression.** Although high-grade metamorphic rocks are difficult to retrogress, overprinting of peak metamorphic mineral assemblages formed at ultrahigh pressures by lower pressure mineral assemblages commonly occurs, probably facilitated by exsolution of structural OH and molecular $H_2O$ held in nominally anhydrous minerals during exhumation (Zheng, 2009; Chen et al., 2011; Wang et al. 2017). However, even in these retrogressed UHP metamorphic rocks close-to-peak phase assemblages are commonly preserved as inclusions in accessory minerals and have proved to be important for retrieving reliable peak *P*–*T* information from these rocks (Liu and Liou 2011).

**Polymetamorphism.** With the exception of the Archean rock record, based on our literature review for this study polymetamorphism appears to be a relatively rare phenomenon. However, wherever polymetamorphism is suspected it may create ambiguity in the interpretation of the age of the peak metamorphic mineral assemblage and the *P*–*T* conditions achieved. We illustrate this problem with three examples from the dataset for which we have made an interpretation that could turn out to be incorrect (of course, there may be others that could be reinterpreted with new data).

The first example is the Gruf complex in the Central Alps and concerns the age of UHT granulite facies metamorphism, specifically whether it was Permian or Paleogene. Granulites within the complex are clearly polymetamorphic (Galli et al. 2011; Guevara and Caddick 2016). Zircon geochronology has been used to argue that the UHT metamorphism occurred at ca 272

Ma (Galli et al. 2012), whereas both zircon and monazite indicate an age of ca 33 Ma for the amphibolite facies overprint (Liati and Gebauer 2008; Schmitz et al. 2009; Galli et al. 2012). In this study, we have assigned an age of ca 272 Ma to the UHT metamorphism.

The second ambiguity concerns the Belomorian Eclogite Province where are two different types of eclogite—the Salma type in the north (interpreted to be subduction related) and the Gridino type in the south (a series of mafic dikes). The controversy, which applies to both types of eclogite, concerns whether the age of the HP metamorphism was Neoarchean (e.g. Mints et al. 2010; Kaulina et al. 2010; Dokukina et al. 2014; Li et al. 2015) or Paleoproterozoic (e.g. Skublov et al. 2011a, b; Herwartz et al. 2012; Li et al. 2017a, 2017b; Liu et al. 2017). With the exception of the study by Herwartz et al. (2012), which used Lu–Hf garnet geochronology, most studies have used U–Pb zircon geochronology, which has yielded ambiguous results. Similarly, thermobarometry has yielded a wide range of *P*–*T* conditions, likely at least in part due to the strong retrogression recorded in many samples. In this study, we prefer the interpretation that these eclogites are Paleoproterozoic rather than Neoarchean.

Finally, there is a similar problem with the age of eclogite facies metamorphism in the upper deck domain of the Athabasca granulite terrane. In a detailed petrological and geochronological study, Baldwin et al. (2004) interpreted a zircon IDTIMS $^{207}Pb/^{206}Pb$ weighted mean age of ca 1.904 Ga as the time of peak eclogite facies metamorphism. This interpretation was confirmed by in situ analysis of metamorphic zircons that yielded a SHRIMP $^{207}Pb/^{206}Pb$ weighted mean age of ca 1.905 Ga. Based on inclusions of high-pressure minerals and the petrographic setting of these zircons in omphacitic clinopyroxene, Baldwin et al. (2004) linked zircon growth to the eclogite facies metamorphism. However, Dumond et al. (2017) have reinterpreted the age of the eclogite facies metamorphism to be Neoarchean based on new monazite ages from the surrounding paragneisses. Although there is clear and widespread evidence of Neoarchean metamorphism in the Athabasca granulite terrane (Dumond et al. 2015), the original interpretation of the Baldwin et al. (2004) zircon ages has not been refuted to our satisfaction by Dumond et al. (2017). Thus, in this study we prefer the original interpretation that the eclogite facies metamorphism was Paleoproterozoic.

**Preservation and preservation bias.** The rock record is unambiguously incomplete (e.g. there is no significant volume of Hadean crust), leading to uncertainties regarding preservation. For example, it may be suggested that blueschists and UHP metamorphic rocks were not preserved prior to the Cryogenian. However, the absence of evidence is not a scientific argument. The testable hypothesis is that blueschist and UHP metamorphism is a global phenomenon that first appeared in the rock record in the Neoproterozoic; this hypothesis is potentially falsified if an earlier record of blueschist and UHP metamorphism is identified. In this circumstance, the first question to be asked is whether the occurrence records a local or global event, i.e. whether it represents an outlier in a global context or the start of cold subduction globally. There is a caveat in that some protoliths, such as granodiorite and granite typical of the continental crust, may not transform completely during low d$T$/d$P$ metamorphism if they become fluid absent during passage through the high-pressure amphibolite facies (Young and Kylander-Clark 2015).

The question of preservation bias was addressed by Hawkesworth et al. (2009) who argued that the coincidence of peaks of crystallization ages in the continental record with the supercontinent cycle are likely to reflect biases in preservation. Since the crustal record of metamorphism exhibits a similar coincidence with the supercontinent cycle (Brown, 2007, 2014), potential biases in preservation apply equally to the metamorphic rock record. However, this bias does not explain the absence of blueschist metamorphism from the crustal rock record until the late Tonian (Supplementary Data Table—Aksu blueschist terrane, western China) or that UHP metamorphism is a characteristic feature of subduction-to-collision orogenesis during the Phanerozoic (Brown 2014). The widespread appearance of blueschists and UHP eclogites in the rock record during the Cryogenian–Cambrian (0.72 to 0.485 Ga) has been interpreted to register a change to colder subduction and the beginning of the modern plate tectonic regime (Brown 2006, 2007, 2008). This interpretation was supported by the results of experiments using a 2D petrological–thermomechanical numerical model that simulates the processes of oceanic subduction followed by continental collision (Sizova et al. 2014).

## HYPOTHESIS

On contemporary Earth, different plate tectonic settings are characterized by differences in heat flow that are recorded in metamorphic rocks as different apparent thermal gradients. For simplicity in this study, we use the ratio of *T/P* at the assigned *P–T* value, hereafter referred to as thermal gradient. Note that this thermal gradient is not equivalent to the geotherm, or the *P–T* path followed by the rock, or the metamorphic field gradient. Using thermal gradients metamorphic rocks may be classified into three natural groups. For metamorphic rocks of Phanerozoic age, there are relationships between these three different types of metamorphism and plate boundary processes. As a result, the full dataset may be interrogated to determine if there have been secular changes in thermal gradients of metamorphism and to establish how far back into the Precambrian the imprint of global plate tectonics is registered in the metamorphic rock record.

The null hypothesis tested herein states that thermal gradients recorded by metamorphic rocks through time do not vary outside of the range expected for different plate tectonic settings on contemporary Earth. The alternative hypothesis states that secular change in thermal gradients evident in the metamorphic rock record relates to secular change in geodynamic regime. If the null hypothesis is falsified and the alternative hypothesis is accepted, then whether secular change in thermal gradients registers changes in geodynamics and/or the onset of global plate tectonics are topics for discussion.

## TYPES OF METAMORPHISM

Following Brown (2007, 2014), we divide the field of metamorphism into three types based on differences in thermal gradient as listed in the Supplementary Data Table. However, the present dataset includes rocks that are neither granulite nor eclogite, but are schist or gneiss, making the previous terminology used by Brown (2007, 2014), which referred to granulite and eclogite facies metamorphism, inappropriate. Thus, we have changed the terminology to a more general classification, as follows: low d*T*/d*P* (formerly "high-pressure–ultrahigh-pressure metamorphism"); intermediate d*T*/d*P* (formerly "eclogite–high pressure granulite metamorphism"); and, high d*T*/d*P* (formerly "granulite–ultrahigh temperature metamorphism").

The assigned *P*–*T* for each of these types of metamorphism may not be strictly equivalent. Thus, for low d*T*/d*P* metamorphism, *P*–*T* is either the maximum *P*–*T* or the *T* at maximum *P*; for intermediate d*T*/d*P* metamorphism, the maximum *P* and *T* generally occur together; and for high d*T*/d*P* metamorphism, *P*–*T* is either the maximum *P*–*T* or the *P* at maximum *T*. These differences reflect the reality of a dynamic environment during orogenesis where *T* and *P* evolve over time. As discussed earlier, in the case of clockwise *P*–*T*–*t* paths, the evolution is from lower to higher thermal gradients reflecting thickening, heating and exhumation, whereas for counter-clockwise *P*–*T*–*t* paths, the evolution is from higher to lower thermal gradients, reflecting initially hot lithosphere that thickens and cools.

In Fig. 1, the 456 data listed in the Supplementary Data Table are plotted in *P*–*T* space in relation to the range of thermal gradients for each type (Fig. 1a) and the standard metamorphic facies (Fig. 1b; metamorphic facies from Brown 2014). As a result of the increase in size of the dataset, we have modified slightly the range of thermal gradients for each type compared with those used by Brown (2007, 2014). With very few exceptions (discussed below), low d*T*/d*P* metamorphism occurs at thermal gradients < 375 °C/GPa, intermediate d*T*/d*P* metamorphism between thermal gradients of 375 and 775 °C/GPa, and high d*T*/d*P* metamorphism occurs at thermal gradients > 775 °C/GPa (Fig. 1a).

## TEMPERATURES, PRESSURES AND THERMAL GRADIENTS OF METAMORPHISM

The dataset is displayed graphically by type of metamorphism using box and whisker plots for temperature, pressure and thermal gradient, as shown in Fig. 2. These plots show that the three types form distinct populations with close to normal distributions, only limited dispersion and few outliers. For each type, from high d*T*/d*P* to low d*T*/d*P*, the mean temperatures are 843 ± 110 (1σ), 787 ± 109 and 647 ± 149 °C, the mean pressures are 0.79 ± 0.18 (1σ), 1.43 ± 0.35 and 2.68 ± 0.94 GPa, and the mean thermal gradients (d*T*/d*P*) are 1109 ± 251 (1σ), 574 ± 116 and 255 ± 59 °C/GPa, respectively.

There are a small number of outliers for each type. Outliers for *T* and *P* in the high d*T*/d*P* type include the late Paleozoic accretionary wedge of central Chile, which has a low *T* of 555 °C (Supplementary Data Table), the Southern Granulite Terrain of India, which has a high *P* of 1.25

GPa (the Supplementary Data Table) and Badcall Bay in the Lewisian Complex of Scotland, which has a high *P* of 1.4 GPa (the Supplementary Data Table); none of these are outliers in terms of thermal gradient. There are five outliers with anomalously high thermal gradients, all of which record very low-pressures (< 0.55 GPa) and three of which record ultrahigh temperatures (>900 °C). Outliers for *T* and *P* in the intermediate d*T*/d*P* type are the Fada N'Gourma region of Burkina Faso, which has a low *T* of 425 °C (Supplementary Data Table), and three examples of anomalously high *P* (> 2.25 GPa), as follows (Supplementary Data Table): the Alxa area of the northern North China craton; granulite from the borehole at Tirschheim in the Granulitgebirge of Saxony in Germany; and, eclogite and granulite xenoliths from the Dunkeldik magmatic field in the central Pamir Mountains. There are no outliers in terms of thermal gradient. Outliers for *T* and *P* in the low d*T*/d*P* type include two localities with anomalously high *T* (Supplementary Data Table: Kumdy-Kol in the Kokchetav Massif of northern Kazakhstan, and Stráž nad Ohří in the Eger complex of the Czech Republic), one of which also has anomalously high *P* (Kumdy-Kol), and two additional localities with anomalously high *P* (Supplementary Data Table: locality on the north side of Nordre Stromfjord in the Nagssugtoqidian orogen of West Greenland, and Barchi-Kol in the Kokchetav Massif of northern Kazakhstan); none of these are outliers in terms of thermal gradient. The blueschists on Anglesey in Wales record an anomalously high thermal gradient (Supplementary Data Table), which may relate to the fact that they formed along a counter-clockwise *P*–*T*–*t* path (Horsfall 2009).

**The present back to the Neoarchean**

At this point we remind the reader that regional metamorphism is intrinsically a dynamic process during which temperature and pressure evolve with time; our use of a single peak *P*, *T* and *t* for each location is a necessary but simplified numerical characterization of this process. Although we advocate using the apparent thermal gradient (d*T*/d*P*) derived from the metamorphic peak *P*–*T* to characterize each location at the peak age, we recognize that this places limitations on the inferences that may be derived from the dataset. In particular, we note that we are not able to address rates of burial and exhumation with this type of data. Assessing secular change in the rates of these processes is a project for the future, although the interested reader is referred to Dunlap (2000), Willigers et al. (2002), Scibiorski et al. (2015) and Nicoli et al. (2016).

Figure 3 shows temperatures of metamorphism *versus* age. Although widely scattered, temperatures were uniformly high from the Neoarchean to the Paleozoic, but there is a dramatic drop in the temperature of metamorphism with the appearance of HP–UHP metamorphism in the late Tonian. Linear regression of the data shows no significant change with time for temperatures of high and intermediate d*T*/d*P* metamorphism, but a significant decrease in temperatures of low d*T*/d*P* metamorphism (i.e. *p*-values are < or <<0.05). A second order polynomial regression through the data for high d*T*/d*P* metamorphism is statistically meaningful (i.e. *p*-values are < or <<0.05), and suggests that metamorphic temperatures for this type peaked during the Proterozoic (Fig. 3).

Figure 4 shows pressures of metamorphism *versus* age. Pressures were uniformly low (high d*T*/d*P* metamorphism) or moderate (intermediate d*T*/d*P* metamorphism) from the Neoarchean to the Paleozoic, but there is a dramatic increase in recorded pressures with the appearance of HP–UHP metamorphism. Linear regression of the data indicates no statistically significant change in pressure with time for high and low d*T*/d*P* metamorphism, and a slight but significant rise in pressure with time for intermediate d*T*/d*P* metamorphism (Fig. 4).

The extremes of UHT and UHP metamorphism encourage thinking in terms of temperature and pressure, but it is the thermal gradient that is the characteristic feature of different plate boundary tectonic settings on Earth. Thus, there is nothing significant in arbitrarily separating high d$T$/d$P$ metamorphism at temperatures greater than 900 °C or separating low d$T$/d$P$ metamorphism at the quartz to coesite transformation. It is the temporal record of thermal gradients retrieved from crustal rocks that will provide most information about secular change in thermal regimes and, by inference, tectonic settings. Thermal gradients of metamorphism *versus* age are shown in Fig. 5. Linear regression shows no statistically significant change in thermal gradient since the Neoarchean for high d$T$/d$P$ metamorphism, and a slight but significant decrease for both intermediate and low d$T$/d$P$ metamorphism. Similar to the record of temperature, a second order polynomial regression through the data for high d$T$/d$P$ metamorphism is statistically meaningful and suggests that thermal gradients for this type peaked during the interval from 2.2 to 0.8 Ga (Fig. 5).

For high d$T$/d$P$ metamorphism, the maximum in thermal gradients during the interval from 2.2 to 0.8 Ga is confirmed as robust by plotting a moving mean of the data calculated every 1 Myr within a moving 300 Myr window (Fig. 6). However, the structure of these data is more complex. The thermal gradients step up during the early Paleoproterozoic at ca 2.3 Ga reaching a peak between 1.3 Ga and 1.0 Ga, before dropping through the Neoproterozoic to a low in the late Tonian (Fig. 6). Thermal gradients rise again to a secondary peak during the Paleozoic (Fig. 6). By contrast, for intermediate d$T$/d$P$ metamorphism there is less variation in the thermal gradients (Fig. 6). A moving mean of the data calculated every 1 Myr within a moving 300 Myr window steps down by approximately 20 °C/GPa in the early Paleoproterozoic at ca 2.3 Ga and by approximately 40 °C/GPa more in the late-Mesoproterozoic (Ectasian–Stenian). There is a rise of approximately 40 °C/GPa to a broad peak centered on the late Tonian before decreasing again through the Paleozoic–Mesozoic to peak again in the Cenozoic (Fig. 6). Finally, for low d*T*/d*P* metamorphism a moving mean of the thermal gradients calculated every 1 Myr within a moving 100 Myr window decreases by approximately 50 °C/GPa from ~300 °C/GPa in the late Tonian to ~250 °C/GPa in the Lower Devonian (Emsian), thereafter remaining flat through the Mesozoic and Cenozoic (Fig. 6).

## Before the Neoarchean

Before the Neoarchean Era data are sparse. Temperatures of metamorphism do not appear to reach the extremely high values recorded during the post Mesoarchean period (Fig. 3) and pressures are moderate (Fig. 4). The *P*–*T*–*t* paths of two well studied granite-greenstone belts could have been generated by mostly vertical tectonic processes (coupled with crustal convective overturns) related to linked sites of crustal delamination and mantle upwelling (Sizova et al., 2017). However, higher and lower thermal gradients are also recognized (Fig. 5), suggesting the possibility that two contrasting tectonic settings could have been present locally on Earth before the Neoarchean.

## Periodicity in the metamorphic record

Figure 7 shows a histogram and probability curve for the age of metamorphism for the 456 localities from the Supplementary Data Table; the data are not uniformly distributed. There are well-defined age peaks at ca 2.7 Ga, 2.5 Ga, 1.6 Ga, 1.025 Ga and 50 Ma, a broad, noisy peak from 2.0 to 1.8 Ga and a very broad, very noisy peak from 650 to 200 Ma (Fig. 7).

The age peaks in the metamorphic record may be compared with those derived from extensive datasets of zircon ages from detrital sediments and orogenic granitoids. In a study of ~200,000 detrital zircon ages, Voice et al. (2011) identified statistically significant global age peaks at 3.5–3.4 Ga, 2.7–2.5 Ga, 2.0–1.7 Ga, 1.2 –1.0 Ga and 0.7–0.5 Ga. Similarly using detrital zircons from both ancient and modern sediments (*n* ~31,000), and zircons from orogenic granitoids (*n* ~7000), Condie and Aster (2010) identified approximate central ages for peak clusters at 2.7 Ga, 2.5 Ga, 1.87 Ga, 1.0 Ga, 0.6 Ga and 0.3 Ga. In a study of ages from detrital zircons from modern river sediments, Condie et al. (2011) identified a separate age peak at 1.6 Ga comparable to that in the metamorphic ages. These age distributions are likely correlated and controlled by the amalgamation of continental fragments into supercratons in the late Archean (Bleeker 2003) and supercontinents during the Proterozoic and Phanerozoic (cf. Voice et al. 2011; Condie and Aster 2010; Condie et al. 2011). The period tripling identified by Puetz et al. (2017) in a large global U–Pb zircon age dataset (>400,000 ages)—at ca 91 myr, ca 273 myr and ca 819 myr—is cryptic in the metamorphic ages, although the two intervals from the appearance of the first supercratons to the amalgamation of Columbia and from Columbia to the amalgamation of Rodinia correspond to the longest period.

The very broad and noisy age peak at 650–200 Ma in the record of metamorphic ages suggests a greater complexity to convergent plate interactions in the modern plate tectonic regime driven by deep subduction (Brown 2006). There are three components to the age peak: the Gondwana-forming orogens; the terrane suturing events related to the Caledonides, Variscides and Altaides; and, the final amalgamation of the Laurasia orogenic collage with Gondwana to form Pangea (Stampfli et al., 2013).

**Low d*T*/d*P* and subduction zone *P*–*T* paths**

In Fig. 8 we show *P*–*T* plots for the low d*T*/d*P* data together with modeled subduction zone *P*–*T* paths for close to the top of the subducting slab (150 m depth; purple) and close to the Moho (6.5 km depth; blue) for active subduction zones (Syracuse et al. 2010; updated by P. van Keken, pers. comm., 2016). The data that plot at *P* >2 GPa match well with the range of *P*–*T* paths in the crustal layer of the subducting slab for active subduction zones. At lower pressures, the data plot at higher temperatures than contemporary subduction zones, which may indicate that the *P*–*T* conditions recorded by the peak mineral assemblages reflect heating during the initial stage of exhumation after the highest *P* attained during subduction and decoupling from the downgoing subducting slab. Overall, the similarity between the *P*–*T* data from the rock record of low d*T*/d*P* metamorphism and the range of *P*–*T* paths for contemporary subduction supports the interpretation that this type of metamorphism records evidence of subduction (Stern 2005, Brown 2006).

**A change in geodynamics during the Neoproterozoic?**

In Fig. 9 we plot *P*–*T* data for the 456 localities from the Supplementary Data Table by age, with data older than 0.8 Ga shown in (a) and data younger than 0.8 Ga shown in (b). A comparison of the two plots demonstrates the dramatic change in thermal gradients of metamorphism associated with subduction during the Neoproterozoic transition to the cold subduction style of the Phanerozoic. Brown (2007) attributed this dramatic change to ". . . whole mantle convection as oceanic lithosphere became thicker with decreased thermal gradients" enabling subduction of continental lithosphere to mantle depths and its (partial) return. Subsequently, Sizova et al (2014) used a 2-D petrological–thermomechanical numerical model of continental collision to demonstrate a change from shallow to deep breakoff of the subducting slab as upper mantle temperature declined to <100 °C warmer than the present day during the late Proterozoic. The deeper slab breakoff is due to stronger crust–mantle coupling, which also enables continental lithosphere to be subducted to mantle depths. Both Brown (2007) and Sizova et al. (2014) interpreted this change as registering the beginning of the modern plate tectonic regime. Prior to this change, shallow slab breakoff limited the amount of depression of isotherms associated with subduction. The absence of cold subduction provides an explanation for the absence of low d*T*/d*P* metamorphic rocks, including blueschists, from the geological record until the Neoproterozoic.

## DISCUSSION

Low d*T*/d*P* extends back to the late Tonian globally, with three (local) outliers, one in the Mesoproterozoic and two in the Paleoproterozoic (Fig. 5). Since blueschist and ultrahigh-pressure metamorphic rocks are linked to subduction, Stern (2005) argued that "the modern style of subduction tectonics began in Neoproterozoic time." However, two contrasting types of metamorphism—one with thermal gradients of 375–775 °C/GPa (intermediate d*T*/d*P*), producing eclogite, high pressure granulite and high pressure amphibolite facies rocks, and another with thermal gradients >775 °C/GPa (high d*T*/d*P*), producing upper amphibolite and granulite facies, and ultrahigh temperature metamorphic rocks—are registered widely in the rock record back to ca 2.8 Ga (Fig. 5).

The emergence of 'paired' metamorphism at the end of the Mesoarchean was interpreted by Brown (2006, 2007, 2014) to manifest the onset of one-sided subduction at newly created convergent plate boundaries, where the lower thermal gradients were inferred to be associated

DOI: http://dx.doi.org/10.2138/am-2018-6166

with the subduction-to-collision suture and the higher thermal gradients with the hinterland in the overriding plate. The frequency of occurrences since 2.8 Ga compared with the paucity prior to 2.8 Ga suggests that a fully linked network of mobile belts had formed by this time completing the transition to a global plate tectonics geodynamic regime. Although we are cognizant that such a change in frequency of occurrences could relate to the better preservation of continental crust as the Earth begins to cool after 3.0 Ga (Labrosse and Jaupart 2007), an interpretation that this change records the onset of global plate tectonics is consistent with some numerical models of the development of plate tectonics (e.g. Bercovici and Ricard 2014). Furthermore, 3.0–2.8 Ga is the time at which there is a significant increase in the number of zircons preserved from continental crust (Condie et al. 2011; Voice et al. 2011) as well as an apparent change in the proportion of juvenile additions to the crust *versus* reworking of pre-existing crust (Dhuime et al. 2012, 2016; Hawkesworth et al. 2016; Tang et al. 2016). This change may record the first appearance of continental arcs above subduction zones in the nascent plate tectonic regime.

The progressive appearance of blueschists and low-temperature eclogites in the global rock record during the interval from the late Tonian to the early Cambrian was interpreted by Brown (2006) to reveal a change to lower d$T$/d$P$ during subduction, probably generated by deeper slab breakoff, which also enabled subduction of continental lithosphere to mantle depths (Sizova et al. 2014). The suggestion that the emergence of blueschists on Earth was linked to secular change in oceanic crust composition (Palin & White 2016) is unlikely, as there is no evidence of significant secular variation in the MgO content of greenstone basalts since the Mesoarchean (Condie et al. 2016). The major element compositions of low MgO greenstone basalts are appropriate to have generated blueschists; the absence of these rocks in the Archean implies that an appropriate tectonic setting was not available. Importantly, the low MgO

DOI: http://dx.doi.org/10.2138/am-2018-6166

greenstone basalts provide an appropriate source for the widespread tonalite–trondhjemite–granodiorite suites that dominate Archean crust (Johnson et al. 2014, 2017). We emphasize that it is the progressive appearance of both blueschists and low-temperature eclogites in the rock record since the late Neoproterozoic that identifies the change to cold subduction globally.

There is a locality on the north side of Nordre Stromfjord in the Nagssugtoqidian orogen (Glassley 2014) that is extraordinary because of its Paleoproterozoic age (ca 1.85 Ga), extreme *P*–*T* conditions (6.95 GPa and 980 °C) and very low thermal gradient (~140 °C/GPa). With a similar age of 1.83 Ga, Weller and St-Onge (2017) have recently reported the occurrence of UHP eclogite in the Paleoproterozoic Trans-Hudson orogen of the Canadian Shield, for which calculated peak metamorphic conditions are 2.50 GPa and 735 °C, which yields d*T*/d*P* of ~295 °C/GPa (Weller and St-Onge 2017). These results are intriguing. However, whether these two occurrences of low d*T*/d*P* type metamorphism in the Paleoproterozoic are local anomalies unique to the Laurentian domain or global markers remains to be seen. One possibility is that geographic patterns of variations in the Earth's mantle have endured since the start of plate tectonics as a direct result of whole-mantle convection within largely isolated cells (Barry et al. 2017). If true, the Laurentian mantle domain may have been colder then other domains since early Archean and the conclusion of Weller and St-Onge (2017) that there may not be a distinction between the Proterozoic and Phanerozoic Eons in terms of metamorphic style may not apply globally.

## SPECULATIONS ABOUT GEODYNAMICS

Insight about the geodynamic history of the Earth may be gleaned from the pattern of secular change in the thermal gradients of high d*T*/d*P* metamorphism in combination with the age distribution of metamorphic rocks of all types, as summarized in Fig. 10. Although there is significant uncertainty in the moving mean of the thermal gradients (Fig. 6), we propose that Earth has evolved through three geodynamic cycles since the Mesoarchean and has just entered a fourth (Fig. 10).

The first cycle extended from the Mesoarchean until the early Paleoproterozoic at ca 2.3 Ga (Fig. 10, Cycle I). Cycle I began with the widespread appearance of two contrasting types of metamorphism in the rock record during the late Mesoarchean and the amalgamation of continental lithosphere terranes into supercratons (Bleeker 2003). This is also the period during which the mantle began to cool as total surface heat flux exceeded internal heat production for the first time (Labrosse and Jaupart 2007; Korenaga 2008; Ganne and Feng 2017). Cycle I was terminated by the breakup of the supercratons into protocontinents during the Siderian–Rhyacian (Bleeker 2003; Ernst et al. 2013).

The second cycle includes the reamalgamation of these protocontinents into the first supercontinent—Columbia/Nuna (hereafter Columbia)—in the mid Paleoproterozoic and extends to the breakup of its closely related successor supercontinent—Rodinia—in the Tonian (Fig. 10, Cycle II). Cycle II began at the rise in thermal gradients of high d$T$/d$P$ metamorphism around 2.3 Ga. The stepwise formation of Columbia via amalgamation of the protocontinents into several large landmasses that ultimately collided to form a coherent supercontinent (Pisarevsky et al. 2014) is recorded by the spread of metamorphic ages from 2.1 to 1.5 Ga (Fig. 10). During the Mesoproterozoic, the thermal gradients of high d$T$/d$P$ metamorphism rose to a maximum (Fig. 10), reflecting insulation of the mantle beneath the quasi-integral continental lithosphere of Columbia, prior to the reorganization of the Columbia geography into the Rodinia geography. As discussed below, this change in geography involved less disruption than the reconfiguration from supercratons to the first supercontinent at the transition from Cycle I to Cycle II (Roberts 2013; Pisarevsky et al. 2014; Roberts et al. 2015).

Cycle II coincides with the age span of most of Earth's anorogenic magmatism (1.9–1.0 Ga; Parnell et al. 2012) and with a scarcity of passive margins in the geological record (Bradley 2008). This period of stability, which has been informally termed the 'boring' billion (1.85–0.85 Ga; Holland 2006) or labeled Earth's middle age (Cawood and Hawkesworth 2014), is sandwiched between two periods of environmental change, both of which saw a rise in atmospheric oxygen and oxygenation of the oceans—at 2.45–1.85 Ga and 0.85–0.54 Ga (Holland 2006).

These two periods of environmental change correlate with the formation of Columbia and the breakup of Rodinia. However, there is much uncertainty concerning whether all of the protocontinents were included in either supercontinent (Pisarevsky et al. 2014) and how much the first supercontinent was fragmented during the late Mesoproterozoic change in geography to the second (Evans 2013). Both geological and palaeomagnetic evidence indicate that Columbia likely remained a coherent continental domain until ca 1.3 Ga. Large dyke swarms with a wide temporal and spatial range are evidence of numerous break-up attempts during the lifespan of Columbia (Ernst et al. 2013). However, these attempts at breakup were not completely successful with some larger continental landmasses, such as those comprising Laurentia, Baltica and Siberia, and an East Gondwana group of Australian and Antarctican cratons, retaining a coherent geography from one supercontinent to the next, although these two landmasses were probably separated by an ocean (Meert 2014; Pisarevsky et al. 2014).

The overall stability of the mid-Proterozoic continental lithosphere is reflected in the development of a long-lived accretionary orogen along the margin of Columbia, from Laurentia

This is a preprint, the final version is subject to change, of the American Mineralogist (MSA)
Cite as Authors (Year) Title. American Mineralogist, in press.
DOI: http://dx.doi.org/10.2138/am-2018-6166

to Amazonia, which was transformed into a collisional orogen during the transformation from Columbia to Rodinia (Roberts 2013). This evolution is reflected in the global Hafnium isotope record, which shows more juvenile compositions while Columbia remained a coherent entity but more evolved compositions during the transition to Rodinia before reverting back to more juvenile compositions in the Neoproterozoic (Gardiner et al. 2016).

One intriguing feature of this period is the apparent deficit in the amount of preserved continental crust. The present estimated volumes of continental crust by Eon/Era are: Archean – $8 \times 10^8$ km$^3$; Paleoproterozoic – $14 \times 10^8$ km$^3$; Mesoproterozoic – $6 \times 10^8$ km$^3$; Neoproterozoic – $12 \times 10^8$ km$^3$; and, Phanerozoic – $28 \times 10^8$ km$^3$ (Walter Mooney, pers, comm. September 2017). To make these data comparable, we have divided these volumes by the length of each Eon/Era, which yields the following results: Archean – $5 \times 10^5$ km$^3$ myr$^{-1}$; Paleoproterozoic – $2 \times 10^6$ km$^3$ myr$^{-1}$; Mesoproterozoic – $1 \times 10^6$ km$^3$ myr$^{-1}$; Neoproterozoic – $2 \times 10^6$ km$^3$ myr$^{-1}$; and, Phanerozoic – $5 \times 10^6$ km$^3$ myr$^{-1}$. Given the similar volumes of preserved crust per unit time during the Paleoproterozoic and Neoproterozoic, one interpretation of the lower volume of preserved crust per unit time during the intervening Mesoproterozoic Era is that less crust was produced. This is consistent with a relatively stable association of continental lithosphere between the assembly of Columbia and the breakup of Rodinia. By contrast, the higher volumes of preserved crust per unit time during the Paleoproterozoic and Neoproterozoic could relate to subduction and arc magmatism prior to and during the amalgamation of Columbia and Gondwana, respectively.

The third cycle is characterized by a steep decline during the Tonian (1.0 to 0.72 Ga) in the thermal gradients of high d$T$/d$P$ metamorphism to their lowest value (Fig. 10) and the appearance of low d$T$/d$P$ metamorphism in the rock record (Fig. 5). We relate the significant drop in thermal gradients for high d$T$/d$P$ metamorphism to the fragmentation of Rodinia

(Merdith et al. 2017). This breakup was associated with unusually extensive continental flood basalt magmatism that not only dominated the global silicate weathering feedback and continental chemical fluxes to the oceans but also led to extraordinary climatic and geochemical perturbations during the Cryogenian and Ediacaran Periods (0.72 to 0.541 Ga; Cox et al. 2016). By contrast, the appearance of low d*T*/d*P* metamorphism (Brown 2006) is consequent upon a change to deeper subduction related to secular cooling of the mantle (Sizova et al. 2014). This change led to the most evolved Hf isotope compositions recorded in continental crust associated with the amalgamation of the Gondwanan landmass in the Ediacaran–Cambrian (Gardiner et al. 2016). In cycle III, thermal gradients for high d*T*/d*P* metamorphism show a rise to a peak at the end of the Variscides during the formation of Pangea, before another steep decline coincides with the breakup of Pangea and the beginning of a fourth cycle at 0.175 Ga (Fig. 10).

Prior to 2.8 Ga the crust registers moderate thermal gradients in both 'high-grade' gneiss terranes and 'low-grade' greenstone belts, with only sporadic occurrences of higher d*T*/d*P* metamorphism and rare examples of lower d*T*/d*P* metamorphism, although reliable quantitative data are limited (Fig. 5). This pattern may reflect a stagnant–deformable lid tectono-magmatic regime in which occurrences of lower d*T*/d*P* metamorphism record local episodes of initiation of subduction and collision rather than formation of a globally continuous network of plate boundaries (Sizova et al. 2015, 2017). The change from a stagnant–deformable lid tectono-magmatic regime to a mobile-lid plate tectonic regime appears to be related to the beginning of secular cooling of the mantle (Sizova et al. 2010), which facilitated a transition to global subduction registered by the appearance of 'paired' metamorphism in the rock record during the late Mesoarchean. This transition may have been diachronous given differences in the timing of supercontinent formation (Bleeker 2003; Ernst and Bleeker 2010). Although the mechanism by which subduction started and plate boundaries evolved remains uncertain (Bercovici and Ricard 2014; Gerya et al. 2015), based on the metamorphic record the onset of plate tectonics probably occurred in the Mesoarchean.

## ACKNOWLEDGEMENTS

We thank Keith Putirka for the invitation to contribute this Centennial review and his patience in waiting for it to finally be submitted sixteen months later than originally promised. We are grateful for reviews by Alan Collins and Simon Harley, and editorial comments from Sandra Piazolo, which helped to improve the content and presentation of this article. This article is a contribution to IGCP 648.

## REFERENCES CITED

Abers, G.A., Nakajima, J., van Keken, P.E., Kita, S., and Hacker, B.R. (2013) Thermal–petrological controls on the location of earthquakes within subducting plates. Earth and Planetary Science Letters, 369, 178–187.

Baldwin, J.A., Bowring, S.A., Williams, M.L., and Williams, I.S. (2004) Eclogites of the Snowbird Tectonic Zone: Petrological and U-Pb geochronological evidence for Paleoproterozoic high-pressure metamorphism in the western Canadian Shield: Contributions to Mineralogy and Petrology, 147, 528–548.

Barry, T.L., Davies, J.H., Wolstencroft, M., Millar, I.L., Zhao, Z., Jian, P., Safonova, I., and Price, M. (2017) Whole-mantle convection with tectonic plates preserves long-term global patterns of upper mantle geochemistry. Scientific Reports, 7, 1870, DOI: 10.1038/s41598-017-01816-y

Bercovici, D., and Ricard, Y. (2014) Plate tectonics, damage and inheritance. Nature, 508, 513–516.

Bleeker, W. (2003) The late Archean record: a puzzle in ca. 35 pieces. Lithos, 71, 99–134.

Brown, M. (1998a) Unpairing metamorphic belts: *P*–*T* paths and a tectonic model for the Ryoke Belt, southwest Japan. Journal of Metamorphic Geology, 16, 3–22.

Brown, M. (1998b) Ridge-trench interactions and high-*T*–low-*P* metamorphism, with particular reference to the Cretaceous evolution of the Japanese Islands. In: Treloar, P.J. and O'Brien, P.J. (eds) What drives metamorphism and metamorphic reactions. Geological Society, London, Special Publications, 138, 131–163.

Brown, M. (2002). Plate margin processes and 'paired' metamorphic belts in Japan. Comment on "Thermal effects of ridge subduction and its implication for the origin of granitic batholith and paired metamorphic belts" by H. Iwamori. Earth and Planetary Science Letters, 199, 483–492.

Brown, M. (2006) Duality of thermal regimes is the distinctive characteristic of plate tectonics since the Neoarchean. Geology, 34, 961–964.

Brown, M. (2007) Metamorphic conditions in orogenic belts: a record of secular change. International Geology Review, 49, 193–234.

Brown, M. (2008) Characteristic thermal regimes of plate tectonics and their metamorphic imprint throughout Earth history: When did Earth first adopt a plate tectonics mode of behavior? In: When Did Plate Tectonics Begin? Condie, K. and Pease, V. (eds). Geological Society of America Special Paper 440, 97-128.

Brown, M. (2009) Metamorphic patterns in orogenic systems and the geological record. In: Accretionary Orogens in Space and Time. Cawood, P.A. and Kröner, A. (eds). Geological Society, London, Special Publications, 318, 37–74.

Brown, M. (2010) Paired metamorphic belts revisited. Gondwana Research, 18, 46–59.

Brown, M. (2014) The contribution of metamorphic petrology to understanding lithosphere evolution and geodynamics. Geoscience Frontiers, 5, 553–569.

Cawood, P.A. and Hawkesworth, C.J. (2014). Earth's middle age. Geology, 42; 503–506.

Cawood, P.A. and Hawkesworth, C.J. (2015). Temporal relations between mineral deposits and global tectonic cycles. Geological Society, London, Special Publications, 393, pp.9-21.

Cesare, B., and Gomez-Pugnaire, M.T. (2001) Crustal melting in the Alboran domain: Constraints from xenoliths of the Neogene Volcanic Province. Physics and Chemistry of the Earth, Part A: Solid Earth and Geodesy, 26, 255–260.

Chen, R.X., Zheng, Y.F., and Gong, B. (2011) Mineral hydrogen isotopes and water contents in ultrahigh-pressure metabasite and metagranite: constraints on fluid flow during continental subduction-zone metamorphism. Chemical Geology, 281, 103–124.

Chopin, C. (2003) Ultrahigh-pressure metamorphism: tracing continental crust into the mantle. Earth and Planetary Science Letters, 212, 1–14.

Clark, C., Fitzsimons, I.C.W., Healy, D., and Harley, S.L. (2011). How does the continental crust get really hot? Elements, 7, 235–240.

Condie, K.C., and Aster, R.C. (2010) Episodic zircon age spectra of orogenic granitoids: The supercontinent connection and continental growth: Precambrian Research, 180, 227–236.

Condie, K.C., Aster, R.C., and van Hunen, J. (2016) A great thermal divergence in the mantle beginning 2.5 Ga: Geochemical constraints from greenstone basalts and komatiites. Geoscience Frontiers, 7, 543–553.

Condie, K.C., Bickford, M.E., Aster, R.C., Belousova, E., and Scholl, D.W. (2011) Episodic zircon ages, Hf isotopic composition, and the preservation rate of continental crust. Geological Society of America Bulletin, 123, 951–957.

Cox, G.M., Halverson, G.P., Stevenson, R.K., Vokaty, M., Poirier, A., Kunzmann, M., Li, Z-X., Denyszyn, S.W., Strauss, J.V., and Macdonald, F.A. (2016) Continental flood basalt weathering as a trigger for Neoproterozoic Snowball Earth. Earth and Planetary Science Letters, 446, 89–99.

Davies, G.F. (2006) Gravitational depletion of the early Earth's upper mantle and the viability of early plate tectonics. Earth and Planetary Science Letters, 243, 376–382.

Dewey, J.F. (1988) Extensional collapse of orogens. Tectonics, 7, 1123–1139.

de Roever, W.P. (1956) Some differences between post-Paleozoic and older regional metamorphism. Geologie en Mijnbouw, 18, 123–127.

de Roever, W.P. (1965) On the cause of the preferential distribution of certain metamorphic minerals in orogenic belts of different age. Geologische Rundschau, 54, 933–943.

Dhuime, B., Hawkesworth, C.J., Cawood, P.A., and Storey, C.D. (2012) A change in the geodynamics of continental growth 3 billion years ago. Science, 335, 1334–1336.

Dhuime, B., Wuestefeld, A., and Hawkesworth, C.J. (2015) Emergence of modern continental crust about 3 billion years ago. Nature Geoscience, 8, 552–555.

Dobrzhinetskaya, L.F. (2012) Microdiamonds—Frontier of ultrahigh-pressure metamorphism: A review. 21, 207–223.

Dokukina, K.A., Kaulina, T.V., Konilov, A.N., Mints, M.V., Van, K.V., Natapov, L., Belousova, E., Simakin, S.G., and Lepekhina, E.N., 2014. Archaean to Palaeoproterozoic high-grade evolution of the Belomorian eclogite province in the Gridino area, Fennoscandian Shield: geochronological evidence. Gondwana Research, 25, 585–613.

Dabrowski, M., Powell, R., and Podladchikov, Y. (2015) Viscous relaxation of grain-scale pressure variations. Journal of Metamorphic Geology, 33, 859–868.

Dumond, G., Goncalves, P., Williams, M.L., and Jercinovic, M.J. (2015) Monazite as a monitor of melting, garnet growth and feldspar recrystallization in continental lower crust. Journal of Metamorphic Geology, 33, 735–762.

Dumond, G., Williams, M.L., Baldwin, J.A., and Jercinovic, M.J. (2017) Backarc origin for Neoarchean ultrahigh-temperature metamorphism, eclogitization, and orogenic root growth. Geology, 45, 943–946.

Dunlap, W.J. (2000) Nature's diffusion experiment: the cooling-rate cooling-age correlation. Geology, 28, 139–142.

Ellis, D.J., Sheraton, J.W., England, R.N., and Dallwitz, W.B. (1980) Osumilite–sapphirine–quartz granulites from Enderby Land, Antarctica—mineral assemblages and reactions. Contributions to Mineralogy and Petrology, 72, 123–143.

Ernst, R.E., and Bleeker, W. (2010) Large igneous provinces (LIPs), giant dyke swarms, and mantle plumes: significance for breakup events within Canada and adjacent regions from 2.5 Ga to the present. Canadian Journal of Earth Sciences, 47, 695–739.

Ernst, R.E., Bleeker, W., Söderlund, U., and Kerr, A.C. (2013) Large Igneous Provinces and supercontinents: Toward completing the plate tectonic revolution. Lithos, 174, 1–14.

Ernst, W.G. (1971) Metamorphic zonations on presumably subducted lithospheric plates from Japan, California and the Alps. Contributions to Mineralogy and Petrology, 34, 43–59.

Ernst, W.G. (1972) Occurrence and mineralogic evolution of blueschist belts with time. American Journal of Science, 272, 657–668.

Ernst, W.G. (1973) Blueschist metamorphism and *P–T* regimes in active subduction zones. Tectonophysics, 17, 255–272.

Evans, D.A.D. (2013) Reconstructing pre-Pangean supercontinents. Geological Society of America Bulletin, 125, 1735–1751.

Ferri, F., Burlini, L., Cesare, B., and Sassi, R. (2007) Seismic properties of lower crustal xenoliths from El Hoyazo (SE Spain): Experimental evidence up to partial melting. Earth and Planetary Science Letters, 253, 239–253.

Fischer, R., and Gerya, T. (2016) Regimes of subduction and lithospheric dynamics in the Precambrian: 3D thermomechanical modeling. Gondwana Research, 37, 53–70.

Galli, A., Le Bayon, B., Schmidt, M.W., Burg, J.P., Caddick, M.J., and Reusser, E. (2011) Granulites and charnockites of the Gruf Complex: Evidence for Permian ultra-high temperature metamorphism in the Central Alps. Lithos, 124, 17–45.

Galli, A., Le Bayon, B., Schmidt, M.W., Burg, J.P., Reusser, E., Sergeev, S.A., and Larionov, A. (2012) U-Pb zircon dating of the Gruf Complex: disclosing the late Variscan granulitic lower crust of Europe stranded in the Central Alps. Contributions to Mineralogy and Petrology, 163, 353–378.

Ganne, J., and Feng, X. (2017) Primary magmas and mantle temperatures through time. Geochemistry Geophysics Geosystems, 18, 872–888.

Gardiner, N.J., Kirkland, C.L., and Van Kranendonk, M.J. (2016) The juvenile Hafnium isotope signal as a record of supercontinent cycles. Scientific Reports, 6:38503, DOI: 10.1038/srep38503.

Gerya, T. (2014) Precambrian geodynamics: concepts and models. Gondwana Research, 25, 442–463.

Gerya, T. (2015) Tectonic overpressure and underpressure in lithospheric tectonics and metamorphism. Journal of Metamorphic Geology, 33, 785–800.

Gerya, T.V., Connolly, J.A.D., and Yuen, D.A. (2008) Why is terrestrial subduction one-sided? Geology, 36, 43–46.

Gerya, T.V., Stern, R.J., Sobolev, S.V., and Whattam, S.A. (2015) Plate tectonics on the Earth triggered by plume-induced subduction initiation. Nature 527, 221–225.

Glassley, W.E., Korstgard, J.A., Sorensen, K., and Platou, S.W. (2014) A new UHP metamorphic complex in the ~1.8 Ga Nagssugtoqidian Orogen of West Greenland. American Mineralogist, 99, 1315–1334.

Godard, G. (2001) Eclogites and their geodynamic interpretation: a history. Journal of Geodynamics, 32, 165–203.

Goldfarb, R. J., Bradley, D. and Leach, D. L. (2010). Secular variation in economic geology. Economic Geology, 105, 459-465.

Grambling, J.A. (1975) Pressures and temperatures in Precambrian metamorphic rocks. Earth and Planetary Science Letters, 53, 63–68.

Green II, H.W., and Burnley, P.C. (1989) A low self-organizing mechanism for deep-focus earthquakes. Nature, 341, 733–737.

Gregoire, M., Mattielli, N., Nicollet, C., Cottin, J.Y., Leyrit, H., Weis, D., Shimizu, N., and Giret, A. (1994) Oceanic mafic granulite xenoliths from the Kerguelen archipelago. Nature, 367, 360–363.

Griffin, W.L., Belousova, E.A., O'Neill, C., O'Reilly, S.Y., Malkovets, V., Pearson, N.J., Spetsius, S., and Wilde, S.A. (2013) The world turns over: Hadean–Archean crust–mantle evolution. Lithos, 189, 2–15.

Griffin, W.L., Afonso, J.C., Belousova, E.A., Gain, S.E., Gong, X.-H., González-Jiménez, J.M., Howell, D., Huang, J.-X., McGowan, N., Pearson, N.J., Satsukawa, T., Shi, R., Williams, P., Xiong, Q., Yang, J.-S., Zhang, M., and O'Reilly, S.Y. (2016) Mantle Recycling: Transition Zone Metamorphism of Tibetan Ophiolitic Peridotites and its Tectonic Implications. Journal of Petrology, 57, 655–684.

Guevara, V.E., and Caddick, M.J. (2016) Shooting at a moving target: phase equilibria modelling of high-temperature metamorphism. Journal of Metamorphic Geology, 34, 209–235.

Hacker, B.R., Peacock, S.M., Abers, G.A., and Holloway, S.D. (2003) Subduction factory – 2. Are intermediate-depth earthquakes in subducting slabs linked to metamorphic dehydration reactions? Journal of Geophysical Research – Solid Earth, 108, Article Number: 2030.

Harley, S.L. (1998) On the occurrence and characterisation of ultrahigh-temperature (UHT) crustal metamorphism. In: P.J. Treloar and P.J. O'Brien, Eds., What Drives Metamorphism and Metamorphic Reactions? 138, 75–101, Geological Society, London, Special Publication.

Harley, S.L. (2008) Refining the *P*–*T* records of UHT crustal metamorphism. Journal of Metamorphic Geology, 26, 125–154.

Hawkesworth, C.J., Cawood, P.A., and Dhuime, B. (2016) Tectonics and crustal evolution. GSA Today, 26, 9, doi: 10.1130/GSATG272A.1.

Hawkesworth, C.J., Cawood, P.A., Kemp, A., Storey, C., and Dhuime, B. (2009) A matter of preservation. Science, 323, 49–50.

Hayob, J.L., Essene, E.J., Ruiz, J., Ortega-Gutiérrez, F., and Aranda-Gómez, J.J. (1989) Young high-temperature granulites from the base of the crust in central Mexico. Nature, 342, 265–268.

Herwartz, D., Skublov, S.G., Berezin, A.V., and Mel'nik, A.E. (2012) First Lu–Hf garnet ages of eclogites from the Belomorian mobile belt (Baltic Shield, Russia). Doklady Earth Sciences, 443, 377–380.

Herzberg, C. (2016) Petrological evidence from Komatiites for an early Earth carbon and water cycle. Journal of Petrology, 57, 2271–2288.

Herzberg, C., Condie, K., and Korenaga, J. (2010) Thermal history of the Earth and its petrological expression. Earth and Planetary Science Letters, 292, 79–88.

Herzberg, C., Asimow, P.D., Arndt, N., Niu, Y., Lesher, C.M., Fitton, J.G., Cheadle, M.J., and Saunders, A.D. (2007) Temperatures in ambient mantle and plumes: constraints from basalts, picrites and komatiites. Geochemistry Geophysics Geosystems 8, Q02006.

Hobbs, B.E., and Ord, A. (2016) Does non-hydrostatic stress influence the equilibrium of metamorphic reactions? Earth-Science Reviews, 163, 190–233.

Hobbs, B.E., and Ord, A. (2017) Pressure and equilibrium in deforming rocks. Journal of Metamorphic Geology, in press.

Holland, H.D. (2006) The oxygenation of the atmosphere and oceans. Philosophical Transactions of the Royal Society, B 361, 903–915.

Horsfall, C. (2009) 40Ar/39Ar Laser probe dating of prograde metamorphism. PhD thesis, University of Manchester, UK.

Hyndman, R.D. (2015) Tectonic consequences of a uniformly hot backarc and why is the Cordilleran mountain belt high? Geoscience Canada, 42, 383–402.

Hyndman, R.D., Currie, C.A., and Mazzotti, S.P. (2005) Subduction zone backarcs, mobile belts, and orogenic heat. GSA Today, 15, 4–10.

Incel, S., Hilairet, N., Labrousse, L., John, T., Deldicque, D., Ferrand, T., Wang, Y., Renner, J., Morales, L., and Schubnel, A. (2017) Laboratory earthquakes triggered during eclogitization of lawsonite-bearing blueschist. Earth and Planetary Science Letters, 459, 320–331.

Isacks, B., Oliver, J., and Sykes (1968) Seismology and new global tectonics. Journal of Geophysical Research, 73, 5855–5899.

Jackson, J., McKenzie, D., Priestley, K., and Emmerson, B. (2008) New views on the structure and rheology of the lithosphere. Journal of the Geological Society, 165, 453–465.

Jaupart, C., Mareschal, J.-C., and Iarotsky, L. (2016) Radiogenic heat production in the continental crust. Lithos, 262, 398–427.

John, T., Medvedev, S., Rüpke, L.H., Andersen, T.B., Podladchikov, Y.Y., and Austrheim, H. (2009) Generation of intermediate-depth earthquakes by self-localizing thermal runaway. Nature Geoscience, 2, 137–140.

Johnson, T.E., Brown, M., Kaus, B., and VanTongeren, J.A. (2014) Delamination and recycling of Archaean crust caused by gravitational instabilities. Nature Geoscience, 7, 47–52.

Johnson, T.E., Brown, M., Gardiner, N.J., Kirkland, C.L. and Smithies, R.H. (2017) Earth's first stable continents did not form by subduction. Nature, 543, 239–243.

Johnson, T.E., Kirkland, C.L., Reddy, S.M., and Fischer, S. (2015) Grampian migmatites in the Buchan Block, NE Scotland. Journal of Metamorphic Geology, 33, 695–709.

Jull, M., and Kelemen, P.B. (2001) On the conditions for lower crustal convective instability. Journal of Geophysical Research – Solid Earth, 106, 6423–6446.

Kadarusman, J., Maruyama, S., Kaneko, Y., Ota, T., Ishikawa, A., Sopaheluwakan, J., and Omori, S. (2010) World's youngest blueschist belt from Leti Island in the non-volcanic Banda outer arc of Eastern Indonesia. Gondwana Research, 18, 189–204.

Kaulina, T.V., Yapaskurt, V.O., Presnyakov, S.L., Savchenko, E.E., and Simakin, S.G. (2010) Metamorphic evolution of the Archean eclogite-like rocks of the Shirokaya and Uzkaya Salma area (Kola Peninsula): Geochemical features of zircon, composition of inclusions, and age. Geochemistry International, 48, 871–890.

Katayama, I., and Maruyama, S. (2009) Inclusion study in zircon from ultrahigh-pressure metamorphic rocks in the Kokchetav massif: an excellent tracer of metamorphic history. Journal of the Geological Society, 166, 783–796.

Kelsey, D.E., and Hand, M. (2014) On ultrahigh temperature crustal metamorphism: Phase equilibria, trace element thermometry, bulk composition, heat sources, timescales and tectonic settings. Geoscience Frontiers, 6, 311–356.

Kirby, S.H., Durham, W.B., and Stern, L.A. (1991) Mantle phase changes and deep earthquake faulting in subducting lithosphere. Science, 252, 216–225.

Kirby, S.H., Stein, S., Okal, E.A., and Rubie, D.C. (1996) Metastable mantle phase transformations and deep earthquakes in subducting oceanic lithosphere. Reviews of Geophysics, 34, 261–306.

Kohn, M.J. (2016) Metamorphic chronology – a tool for all ages: Past achievements and future prospects. American Mineralogist, 101, 25–42.

Kohn, M.J., Corrie, S.L., and Markley, C. (2015) The fall and rise of metamorphic zircon. American Mineralogist, 100, 897–908.

Korhonen, F.J., Clark, C., Brown, M., and Taylor, R. (2014) Taking the temperature of Earth's hottest crust. Earth and Planetary Science Letters, 408, 341–354.

Korenaga, J. (2008) Urey ratio and the structure and evolution of Earth's mantle. Reviews of Geophysics, 46, RG2007, doi:10.1029/2007RG000241.

Korenaga, J. (2013) Initiation and evolution of plate tectonics on Earth: theories and observations. Annual Review of Earth and Planetary Sciences, 41, 117–151.

Kylander-Clark, A.R., Hacker, B.R., and Cottle, J.M. (2013) Laser-ablation split-stream ICP petrochronology. Chemical Geology, 345, 99–112.

Labrosse, S., and Jaupart, C. (2007) Thermal evolution of the Earth: secular changes and fluctuations of plate characteristics. Earth and Planetary Science Letters 260, 465–481.

Li, S.H., Unsworth, M.J., Booker, J.R., Wei, W.B., Tan, H.D., and Jones, A.G. (2003) Partial melt or aqueous fluid in the mid-crust of Southern Tibet? Constraints from INDEPTH magnetotelluric data. Geophysical Journal International, 153, 289–304.

Li, X., Zhang, L., Wei, C., and Slabunov, A.I. (2015) Metamorphic PT path and zircon U–Pb dating of Archean eclogite association in Gridino complex, Belomorian province, Russia. Precambrian Research, 268, 74–96.

Li, X., Yu, H.L., Zhang, L., Wei, C., and Bader, T. (2017a) 1.9 Ga eclogite from the Archean-Paleoproterozoic Belomorian Province, Russia. Science Bulletin, 62, 239–241.

Li, X., Zhang, L., Wei, C., Slabunov, A.I., and Bader, T. (2017b) Neoarchean–Paleoproterozoic granulite-facies metamorphism in Uzkaya Salma eclogite-bearing mélange, Belomorian Province (Russia). Precambrian Research, 294, 257–283.

Liati, A., and Gebauer, D. (2003) Geochronological constraints of the time of metamorphism in the Gruf Complex (central Alps) and implications for the Adula-Cima Lunga Nappe system: Schweizerische Mineralogische und Petrographische Mitteilungen, 83, 159–172.

Liou, J.G., Maruyama, S., Wang, X., and Graham, S. (1990) Precambrian blueschist terranes of the world. Tectonophysics, 181, 97–111.

Liou, J.G., Tsujimori, T., Yang, J.S., Zhang, R.Y., and Ernst, W.G. (2014) Recycling of crustal materials through study of ultrahigh-pressure minerals in collisional orogens, ophiolites, and mantle xenoliths: A review. Journal of Asian Earth Sciences, 96, 386–420.

Liu, F.L, and Liou, J.G. (2011) Zircon as the best mineral for P-T-time history of UHP metamorphism: A review on mineral inclusions and U-Pb SHRIMP ages of zircons from the Dabie–Sulu UHP rocks. Journal of Asian Earth Sciences, 40, 1–39.

Liu, F., Zhang, L., Li, X., Slabunov, A.I., Wei, C., and Bader, T. (2017) The metamorphic evolution of Paleoproterozoic eclogites in Kuru-Vaara, northern Belomorian Province, Russia: Constraints from P-T pseudosections and zircon dating. Precambrian Research, 289, 31–47.

Liu, L., Zhang, J.-F., Green II, H.W., Jin, Z.-M., and Bozhilov, K.N. (2007) Evidence of former stishovite in metamorphosed sediments, implying subduction to > 350 km. Earth and Planetary Science Letters, 263, 180–191.

Lucassen, F., and Franz, G. (1996) Magmatic arc metamorphism: Petrology and temperature history of metabasic rocks in the Coastal Cordillera of northern Chile. Journal of Metamorphic Geology, 14, 249–265.

Maekawa, H., Shozui, M., Ishii, T., Fryer, P., and Pearce, J.A. (1993) Blueschist metamorphism in an active subduction zone. Nature, 364, 520–523.

Maggi, A., Jackson, J., McKenzie, D., and Priestley, K. (2000) Earthquake focal depths, effective elastic thickness, and the strength of the continental lithosphere. Geology, 28, 495–498.

Mancktelow, N.S. (1995) Nonlithostatic pressure during sediment subduction and the development and exhumation of high-pressure metamorphic rocks. Journal of Geophysical Research–Solid Earth, 100, 571–583.

Mancktelow, N.S. (2008) Tectonic pressure: Theoretical concepts and modelled examples. Lithos, 103, 149–177.

Maruyama, S., and Liou, J.G. (1998) Initiation of ultrahigh-pressure metamorphism and its significance on the Proterozoic–Phanerozoic boundary. The Island Arc, 7, 6–35.

Maruyama, S., and Liou, J.G. (2005) From snowball to Phanerozoic Earth: International Geology Review, 47, 775–791.

Maruyama, S., Liou, J. G., and Terabayashi, M. (1996) Blueschists and eclogites of the world and their exhumation. International Geology Review, 38, 490–596.

McCuaig, T.C., and Kerrich, R. (1998) P-T-t-deformation-fluid characteristics of lode gold deposits: evidence from alteration systematics. Ore Geology Reviews, 12, 381–453.

Meert, J.G. (2014) Strange attractors, spiritual interlopers and lonely wanderers: the search for pre-Pangean supercontinents. Geoscience Frontiers, 5, 155–166.

Merdith, A.S., Collins, A.S., Williams, S.E., Pisarevsky, S., Foden, J.D., Archibald, D.B., Blades, M.L., Alessio, B.L., Armistead, S., Plavsa, D., Clark, C., and Müller, R.D. (2017) A full-plate global reconstruction of the Neoproterozoic. Gondwana Research, in press.

Mints, M.V., Belousova, E.A., Konilov, A.N., Natapov, L.M., Shchipansky, A.A., Griffin,W.L., O'Reilly, S.Y., Dokukina, K.A., and Kaulina, T.V. (2010) Mesoarchean subduction processes: 2.87 Ga eclogites from the Kola Peninsula, Russia. Geology 38, 739–742.

Miyashiro, A. (1961) Evolution of metamorphic belts. Journal of Petrology, 2, 277–311.

Miyashiro, A. (1973) Paired and unpaired metamorphic belts. Tectonophysics, 17, 241–254.

Nicoli, G., Moyen, J.F., and Stevens, G. (2016) Diversity of burial rates in convergent settings decreased as Earth aged. Scientific Reports, 6, 26359, DOI: 10.1038/srep26359

Ohuchi, T., Lei, X.L., Ohfuji, H., Higo, Y., Tange, Y., Sakai, T., Fujino, K., and Irifune, T. (2017) Intermediate-depth earthquakes linked to localized heating in dunite and harzburgite. Nature Geoscience, 10, 771–776

Okazaki, K., and Hirth, G. (2016) Dehydration of lawsonite could directly trigger earthquakes in subducting oceanic crust. Nature, 530, 81–85.

O'Neill, C., and Debaille, V. (2014) The evolution of Hadean–Eoarchaean geodynamics. Earth and Planetary Science Letters, 406, 49–58.

Oxburgh, E.R. (1990) Some thermal aspects of granulite history. In: (D. Vielzeuf, and Ph. Vidal, Eds, Granulites and Crustal Evolution. p. 569-580. Kluwer Academic Publishers, The Netherlands.

Oxburgh, E.R., and Turcotte, D.L. (1970) Thermal structure of island arcs. Geological Society of America Bulletin, 81, 1665–1688.

Oxburgh, E.R., and Turcotte, D.L. (1971) Origin of paired metamorphic belts and crustal dilation in island arc regions. Journal of Geophysical Research, 76, 1315–1327.

Palin, R.M., and White, R.W. (2016) Emergence of blueschists on Earth linked to secular changes in oceanic crust composition. Nature Geoscience, 9, 60–64.

Perkins III, D., and Newton, R.C. (1981) Charnockite geobarometers based on coexisting garnet–pyroxene–plagioclase–quartz. Nature, 292, 144–146.

Pisarevsky, S.A., Elming, S.Å., Pesonen, L.J., and Li, Z.X. (2014) Mesoproterozoic paleogeography: supercontinent and beyond. Precambrian Research, 244, 207–225.

Powell, R., Guiraud, M., and White, R.W. (2005) Truth and beauty in metamorphic phase equilibria: conjugate variables and phase diagrams. The Canadian Mineralogist, 43, 21–33.

Powell, R., and Holland, T.J.B. (2008) On thermobarometry. Journal of Metamorphic Geology, 26, 155–179.

Puetz, S.J., Ganade, C.E., Zimmermann, U., and Borchardt, G. (2017) Statistical analyses of Global U-Pb Database 2017. Geoscience Frontiers, in press.

Putirka, K. (2016) Rates and styles of planetary cooling on Earth, Moon, Mars, and Vesta, using new models for oxygen fugacity, ferric–ferrous ratios, olivine–liquid Fe-Mg exchange, and mantle potential temperature. American Mineralogist, 101, 819–840.

Reddy, S.M., Kelley, S.P., and Magennis, L. (1997) A microstructural and argon laserprobe study of shear zone development at the western margin of the Nanga Parbat-Haramosh Massif, western Himalaya. Contributions to Mineralogy and Petrology, 128, 16–29.

Reuber, G., Kaus, B.J.P., Schmalholz, S.M., and White, R.W. (2016) Nonlithostatic pressure during subduction and collision and the formation of (ultra)high-pressure rocks. Geology, 44, 343–346.

Rondenay, S., Abers, G.A., and vanKeken, P.E. (2008) Seismic imaging of subduction zone metamorphism. Geology, 36, 275–278.

Rubatto, D., and Hermann, J. (2007) Experimental zircon/melt and zircon/garnet trace element partitioning and implications for the geochronology of crustal rocks. Chemical Geology, 241, 38–61.

Scherer, E.E., Cameron, K.L., Johnson, C.M., Beard, B.L., Barovich, K.M., and Collerson, K.D. (1997) Lu-Hf geochronology applied to dating Cenozoic events affecting lower crustal xenoliths from Kilbourne Hole, New Mexico. Chemical Geology, 142, 63–78.

Schilling, F.R., and Partzsch, G.M. (2001) Quantifying partial melt fraction in the crust beneath the central Andes and the Tibetan plateau. Physics and Chemistry of the Earth, Part A: Solid Earth and Geodesy, 26, 239–246.

Schmitz, S., Möller, A., Wilke, M., Malzer, W., Kannigiesser, B., Bousquet, R., Berger, A., and Schefer, S. (2009). Chemical U-Th-Pb dating of monazite by 3D-Micro X-ray fluorescence analysis with synchrotron radiation. European Journal of Mineralogy, 21, 927–945.

Scibiorski, E., Tohver, E., and Jourdan, F. (2015) Rapid cooling and exhumation in the western part of theMesoproterozoic Albany-Fraser Orogen, Western Australia. Precambrian Research, 265, 232–248.

Silver, P.G., and Behn, M.D. (2008) Intermittent plate tectonics? Science, 319, 85–88.

Sizova, E., Gerya, T., Brown, M., and Perchuk, L.L. (2010) Subduction styles in the Precambrian: insight from numerical experiments. Lithos 116, 209–229.

Sizova, E., Gerya, T., and Brown, M. (2014) Contrasting styles of Phanerozoic and Precambrian continental collision. Gondwana Research, 25, 522–545.

Sizova, E., Gerya, T., Brown, M., and Stüwe, K. (2017) What drives metamorphism in early Archean greenstone belts? Insights from numerical modeling. Tectonophysics, in press.

Sizova, E., Gerya, T., Stüwe, K., and Brown, M. (2015) Generation of felsic crust in the Archean: A geodynamic modeling perspective. Precambrian Research, 27, 198–224.

Skublov, S.G., Astaf'ev, B.Y., Marin, Y.B., Berezin, A.V., Mel'nik, A.E., and Presnyakov, S.L. (2011a). New data on the age of eclogites from the Belomorian mobile belt at Gridino settlement area. Doklady Earth Sciences, 439, 1163–1170.

Skublov, S.G., Berezin, A.V., and Mel'nik, A.E. (2011b) Paleoproterozoic eclogites in the Salma area, Northwestern Belomorian Mobile Belt: composition and isotopic geochronologic characteristics of minerals and metamorphic age. Petrology 19, 470–495.

Sloan, R.A., Jackson, J.A., McKenzie, D., and Priestley, K. (2011) Earthquake depth distributions in central Asia, and their relations with lithosphere thickness, shortening and extension. Geophysical Journal International, 185, 1–29.

Smith, D.C. (1984) Coesite in clinopyroxene in the Caledonides and its implications for geodynamics. Nature, 310, 641–644.

Stampfli, G.M., Hochard, C., Vérard, C., Wilhem, C., and von Raumer, J. (2013) The formation of Pangea. Tectonophysics, 593, 1–19.

Stern, R.J. (2002) Subduction zones. Reviews of Geophysics, 40, article number: 1012, DOI: 10.1029/2001RG000108.

Stern, R.J. (2005) Evidence from ophiolites, blueschists, and ultrahigh-pressure metamorphic terranes that the modern episode of subduction tectonics began in Neoproterozoic time. Geology, 33, 557–560.

Syracuse, E.M., van Keken, P.E., and Abers, G.A. (2010) The global range of subduction zone thermal models. Physics of the Earth and Planetary Interiors, 183, 73–90.

Tajcmanová, L., Vrijmoed, J., and Moulas, E. (2015). Grain-scale pressure variations in metamorphic rocks: implications for the interpretation of petrographic observations. Lithos, 216–217, 338–351.

Tang, M., Chen, K., and Rudnick, R.L. (2016) Archean upper crust transition from mafic to felsic marks the onset of plate tectonics. Science, 351, 372–375.

Taylor, R.J.M., Harley, S.L., Hinton, R.W., Elphick, S., Clark, C., and Kelly, N.M. (2015) Experimental determination of REE partition coefficients between zircon, garnet and melt: a key to understanding high-temperature crustal processes. Journal of Metamorphic Geology, 33, 231–248.

Taylor, R.J.M., Kirkland, C.L., and Clark, C. (2016) Accessories after the facts: Constraining the timing, duration and conditions of high-temperature metamorphic processes. Lithos, 264, 239–257.

Taylor, R., Clark, C., Harley, S., Kylander-Clark, A., Hacker, B., and Kinny, P. (2017) Interpreting granulite facies events through rare earth element partitioning arrays. Journal of Metamorphic Geology, in press.

Tomkins, A.G. (2010) Windows of metamorphic sulfur liberation in the crust: Implications for gold deposit genesis. Geochimica et Cosmochimica Acta, 74, 3246–3259.

Toussaint, G., Burov, E., and Jolivet, L. (2004) Continental plate collision: Unstable vs. stable slab dynamics. Geology, 32, 33–36.

Tsujimori, T., and Ernst, W.G. (2014) Lawsonite blueschists and lawsonite eclogites as proxies for palaeo-subduction zone processes: a review. Journal of Metamorphic Geology, 32, 437–454.

Tsujimori, T., Sisson, V.B., Liou, J.G., Harlow, G.E., and Sorensen, S.S. (2006) Very-low-temperature record of the subduction process: A review of worldwide lawsonite eclogites. Lithos, 92, 609–624.

Turcotte, D.L., and Schubert, G. (2002) Geodynamics, 456 p. Cambridge University Press, New York.

van Hunen, J., and Moyen, J.-F. (2012) Archean subduction: fact or fiction? Annual Review of Earth and Planetary Sciences 40, 195–219.

van Hunen, J., and van den Berg, A. (2008) Plate tectonics on the early Earth: limitations imposed by strength and buoyancy of subducted lithosphere. Lithos, 103, 217–235.

van Keken P.E., Kita, S., and Nakajima, J. (2012) Thermal structure and intermediate-depth seismicity in the Tohoku-Hokkaido subduction zones. Solid Earth, 3, 355–364.

Voice, P.J., Kowalewski, M., and Eriksson, K.A. (2011) Quantifying the timing and rate of crustal evolution: Global compilation of radiometrically dated detrital zircon grains. The Journal of Geology, 119, 109–126.

Wang, S.-J., Wang, L., Brown, M., Piccoli, P.M., Johnson, T.E., Feng, P., Deng, H., Kitajima, K., and Huang, Y. (2017) Fluid generation and evolution during exhumation of deeply subducted UHP continental crust: Petrogenesis of composite granite–quartz veins in the Sulu belt, China. Journal of Metamorphic Geology, DOI: 10.1111/jmg.12248

Weller, O.M., and St-Onge, M.R. (2017) Record of modern-style plate tectonics in the Palaeoproterozoic Trans-Hudson orogeny. Nature Geoscience, 10, 305–311.

Wheeler, J. (2014) Dramatic effects of stress on metamorphic reactions. Geology, 42, 647–650.

DOI: http://dx.doi.org/10.2138/am-2018-6166

Willigers, B.J.A., van Gool, J.A.M., Wijbrans, J.R., Krogstad, E.J., and Mezger, K. (2002) Posttectonic cooling of the Nagssugtoqidian orogen and a comparison of contrasting cooling histories in Precambrian and Phanerozoic orogens. The Journal of Geology, 110, 503–517.

Wilson, J.T. (1965) A new class of faults and their bearing on continental drift. Nature, 207, 343–347.

Yakymchuk, C., and Brown, M. (2014) The behavior of zircon and monazite during open system melting. Journal of the Geological Society, London, 171, 465–479.

Ye, K., Cong, B.L., and Ye, D.N., 2000. The possible subduction of continental material to depths greater than 200 km. Nature, 407, 734–736.

Young, D.J., and Kylander-Clark A.R.C. (2015) Does continental crust transform during eclogite facies metamorphism? Journal of Metamorphic Geology, 33, 331–357.

Zheng, Y.F. (2009) Fluid regime in continental subduction zones: petrological insights from ultrahigh-pressure metamorphic rocks. Journal of the Geological Society, 166, 763–782.

Zhong, R., Brugger, J., Tomkins, A.G., Chen, Y.J., and Li, W.B. (2015) Fate of gold and base metals during metamorphic devolatilization of a pelite. Geochimica et Cosmochimica Acta, 171, 338–352.

## FIGURE CAPTIONS

**FIGURE 1**. *P*–*T* conditions of metamorphism for 456 localities (Supplementary Data Table) grouped by type, with four representative thermal gradients shown in (**a**) and the fields for the standard metamorphic facies shown in (**b**). The three types of metamorphism are high d*T*/d*P* in red, intermediate d*T*/d*P* in green and low d*T*/d*P* in blue. In (**b**), at pressures below coesite stability the facies boundaries are transitional to indicate the control of bulk composition on the change in mineral assemblages from one facies to another. Low-to-moderate pressure facies are: L, low-grade metamorphism, includes the zeolite facies; Gs, greenschist facies; A, amphibolite

DOI: http://dx.doi.org/10.2138/am-2018-6166

facies; G, granulite facies; and, UHT, ultrahigh temperature metamorphism, which is the part of the granulite facies at T > 900 °C. High-to-ultrahigh pressure facies are: B, blueschist facies; E, eclogite facies; HPG, high-pressure granulite facies, which includes the part of the eclogite facies where plagioclase remains stable in some bulk compositions but not in others at common *P*–*T* conditions; and, UHP, ultrahigh pressure metamorphism, which is the part of the eclogite facies at pressures above quartz stability.

**Figure 2**. Tukey box and whisker plots for (**a**) temperature, (**b**) pressure and (**c**) thermal gradient for each type of metamorphism (high d*T*/d*P* in red, intermediate d*T*/d*P* in green and low d*T*/d*P* in blue). The bottom and top of the box are the first and third quartiles of each subset of data, the line inside the box is the median, the ends of the whiskers represent the lowest and highest data still within 1.5 of the interquartile range, and the individual data points represent outliers.

**Figure 3**. Metamorphic temperature for 456 localities (Supplementary Data Table) grouped by type plotted against age. The three types of metamorphism are high d*T*/d*P* in red, intermediate d*T*/d*P* in green and low d*T*/d*P* in blue. The solid lines show linear regressions of the data by type whereas the dashed line shows a second order polynomial regression for the high d*T*/d*P* type (second order polynomial regressions for the intermediate and low d*T*/d*P* types are similar to the linear regressions).

**Figure 4**. Metamorphic pressure for 456 localities (Supplementary Data Table) grouped by type plotted against age. The three types of metamorphism are high d*T*/d*P* in red, intermediate d*T*/d*P* in green and low d*T*/d*P* in blue. The solid lines show linear regressions of the data by type (second order polynomial regressions for the three types are similar to the linear regressions).

This is a preprint, the final version is subject to change, of the American Mineralogist (MSA)
Cite as Authors (Year) Title. American Mineralogist, in press.
DOI: http://dx.doi.org/10.2138/am-2018-6166

**FIGURE 5**. Metamorphic thermal gradient ($T/P$) for 456 localities (Supplementary Data Table) grouped by type plotted against age. The three types of metamorphism are high d$T$/d$P$ in red, intermediate d$T$/d$P$ in green and low d$T$/d$P$ in blue. The solid lines show linear regressions of the data by type whereas the dashed line shows a second order polynomial regression for the high d$T$/d$P$ type (second order polynomial regressions for the intermediate and low d$T$/d$P$ types are similar to the linear regressions).

**FIGURE 6**. Moving mean with one sigma uncertainty of the thermal gradients for high and intermediate d$T$/d$P$ metamorphism calculated every 1Myr within a moving 300 Myr window, and for low d$T$/d$P$ metamorphism calculated every 1Myr within a moving 100 Myr window. The uncertainty envelopes are 1 sigma.

**FIGURE 7**. Histogram and probability curve for the age of metamorphism for the 456 localities used in this study (Supplementary Data Table).

**FIGURE 8**. *P*–*T* conditions for low d$T$/d$P$ metamorphism compared to subduction zone *P*–*T* paths for close to the top of the subducting slab (150 m depth; purple) and close to the Moho (6.5 km depth; blue) for active subduction zones (Syracuse et al. 2010; updated by P. van Keken, pers. comm., 2016). The fields for the four representative thermal gradients in (**a**) and the standard metamorphic facies in (**b**) are from **FIGURE 1**.

**FIGURE 9**. *P*–*T* conditions of metamorphism for 456 localities (Supplementary Data Table) grouped by age, in (a) > 0.800 Ga grouped a follows > 2.800 Ga, 2.800–2.401 Ga, 2.400–2.001 Ga, 2.000–1.601 Ga, 1.600–1.201 Ga and 1.200–0.801 Ga, and in (b) < 0.800 Ga grouped as follows 0.800–0.501 Ga, 0.500–0.201 Ga and < 0.200 Ga, with four representative thermal gradients for reference from **FIGURE 1 (a)**.

**FIGURE 10**. Moving mean of the thermal gradient for high d*T*/d*P* metamorphism (from **FIGURE 6**) and probability curve for the age distribution of metamorphism (from **FIGURE 7**). The three cycles are discussed in the text.

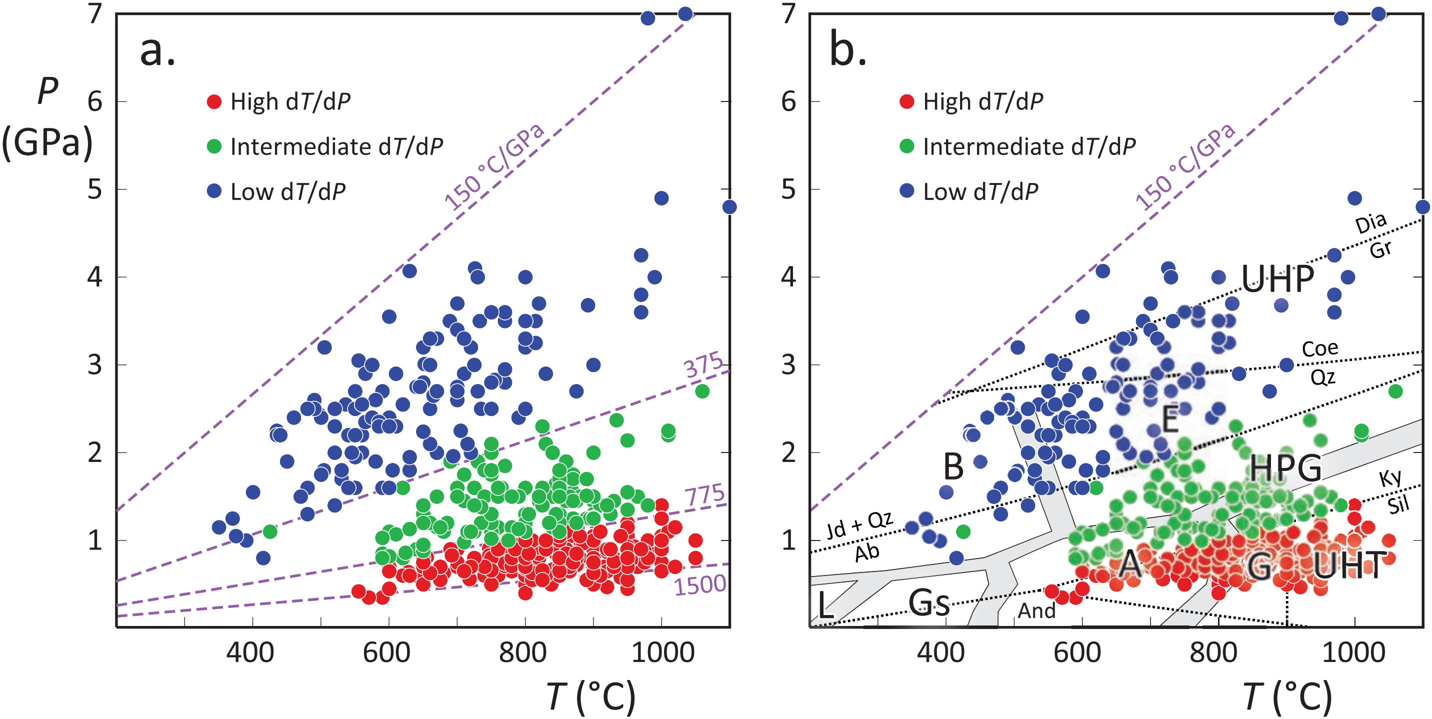
a.
P (GPa)
High dT/dP
Intermediate dT/dP
Low dT/dP
150 °C/GPa
375
775
1500
T (°C)
b.
High dT/dP
Intermediate dT/dP
Low dT/dP
150 °C/GPa
Dia
Gr
UHP
Coe
Qz
E
B
HPG
Ky
Sil
Jd + Qz
Ab
A
G
UHT
L
Gs
And
T (°C)

Figure 1

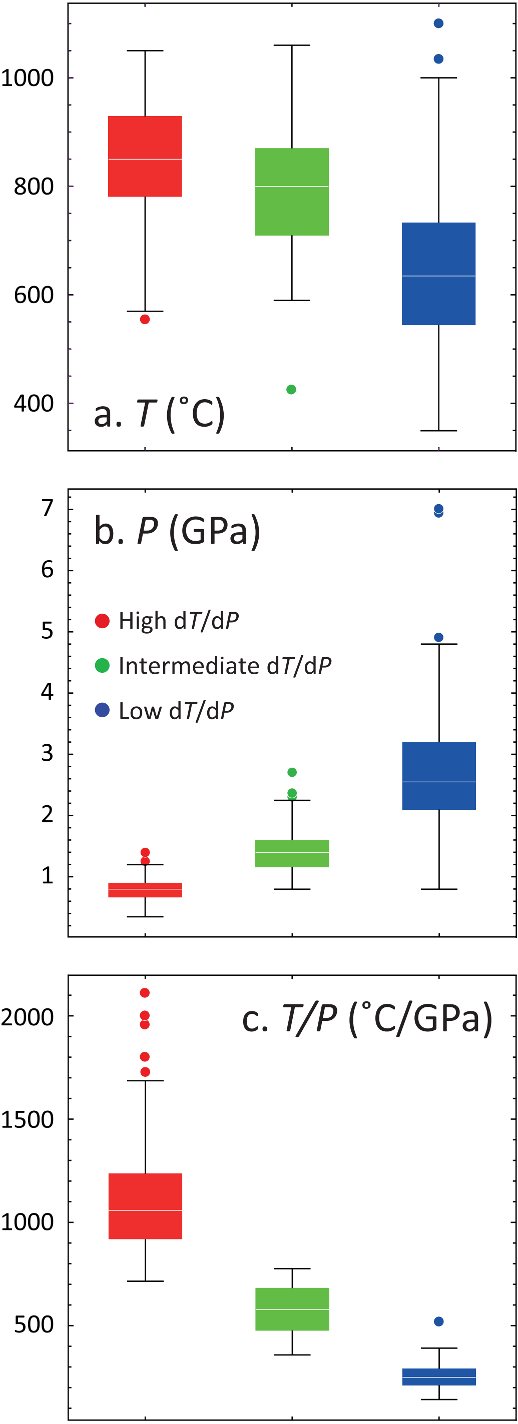

1000
800
600
400
a. T (˚C)
7
6
5
4
3
2
1
b. P (GPa)
High dT/dP
Intermediate dT/dP
Low dT/dP
2000
1500
1000
500
c. T/P (˚C/GPa)


Figure 2

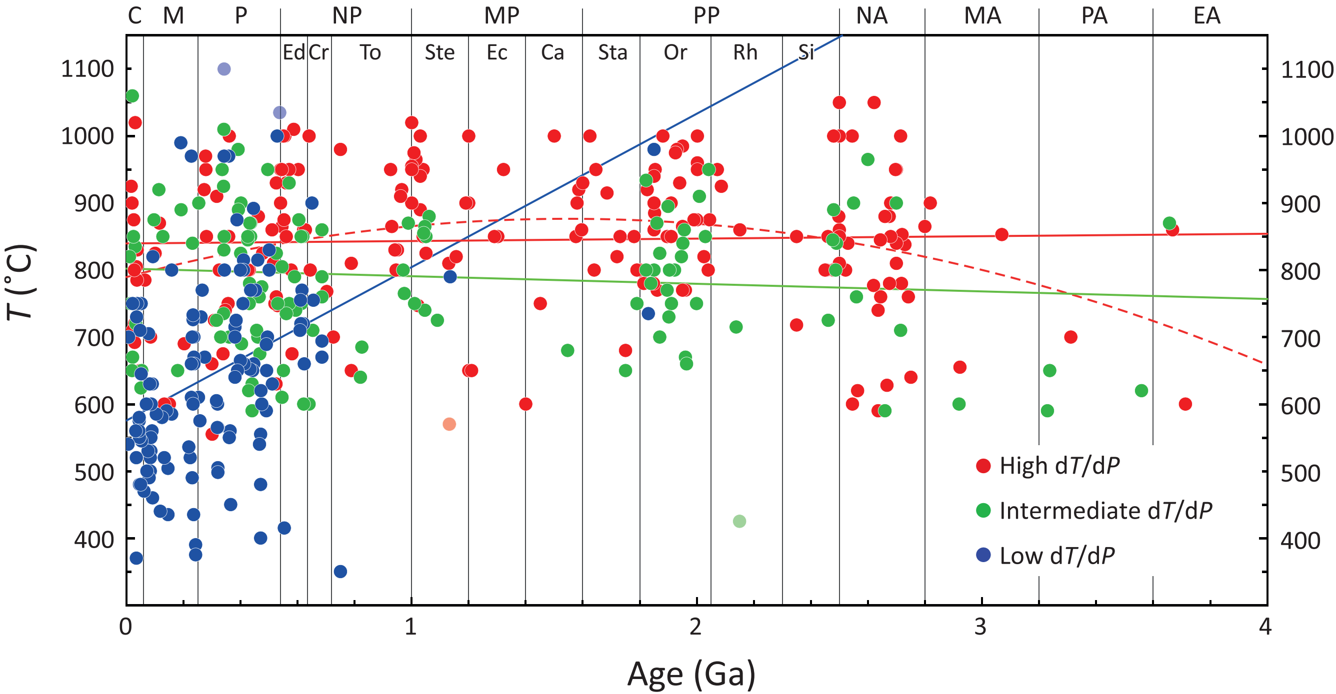
C
M
P
NP
MP
PP
NA
MA
PA
EA
Ed
Cr
To
Ste
Ec
Ca
Sta
Or
Rh
Si
T (°C)
Age (Ga)
High dT/dP
Intermediate dT/dP
Low dT/dP

Figure 3

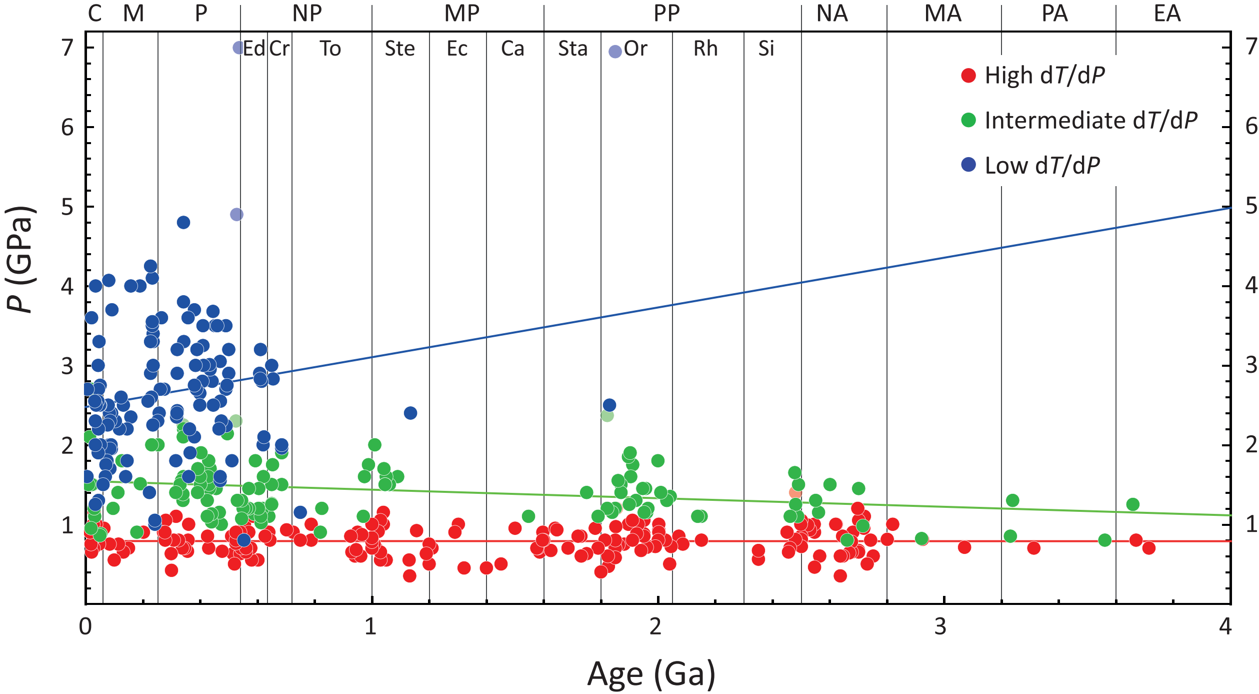

C
M
P
NP
MP
PP
NA
MA
PA
EA
Ed
Cr
To
Ste
Ec
Ca
Sta
Or
Rh
Si
High dT/dP
Intermediate dT/dP
Low dT/dP
P (GPa)
Age (Ga)
0
1
2
3
4
5
6
7


Figure 4

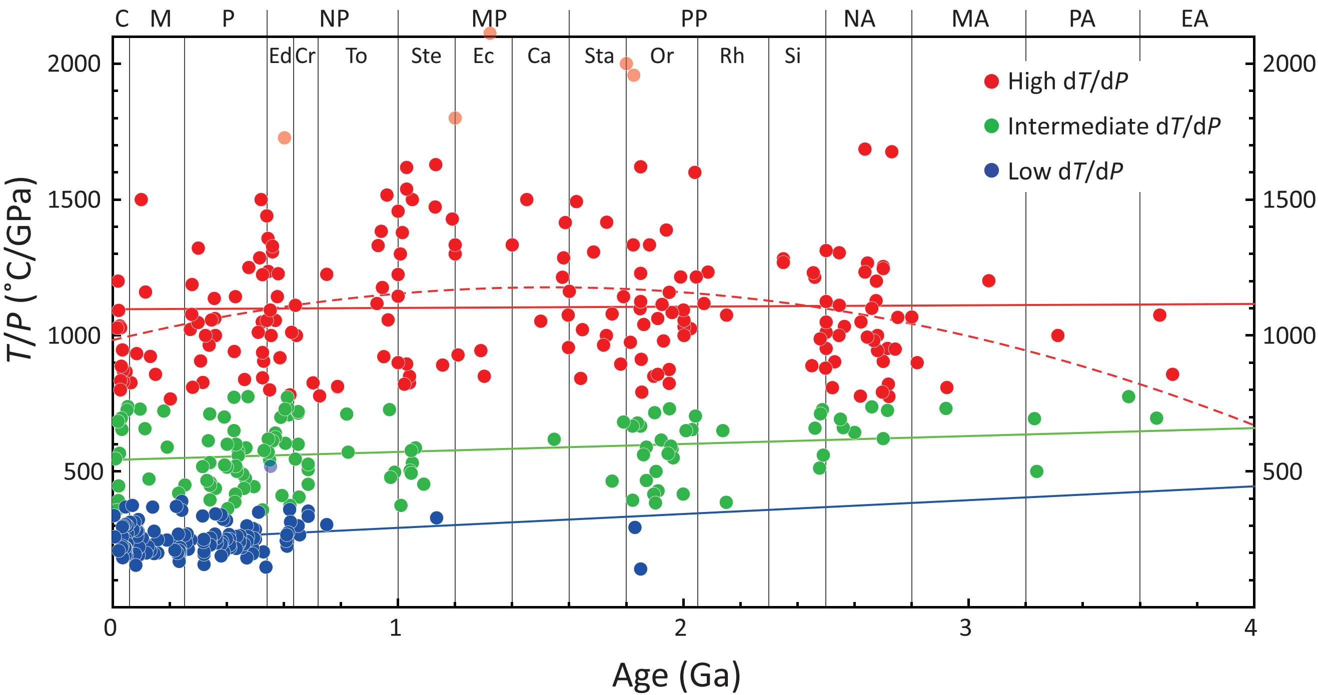

C
M
P
NP
MP
PP
NA
MA
PA
EA
Ed
Cr
To
Ste
Ec
Ca
Sta
Or
Rh
Si
High d$T$/d$P$
Intermediate d$T$/d$P$
Low d$T$/d$P$
$T/P$ (°C/GPa)
2000
1500
1000
500
0
1
2
3
4
Age (Ga)


Figure 5

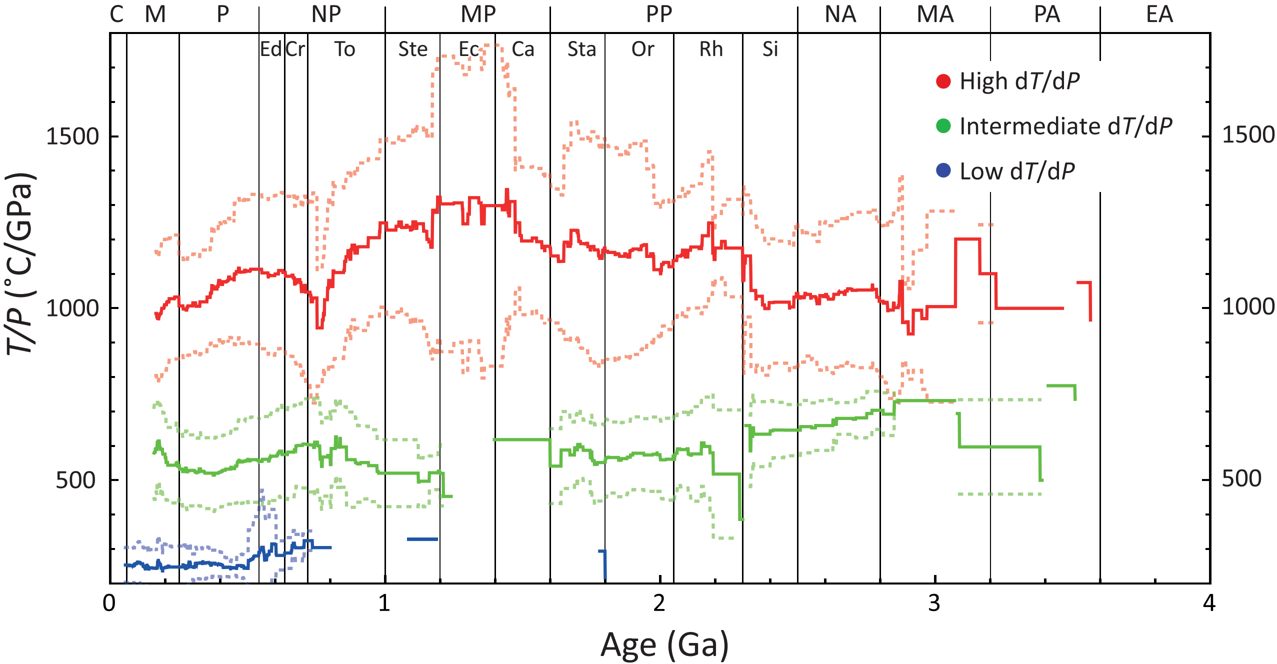

C
M
P
NP
MP
PP
NA
MA
PA
EA
Ed
Cr
To
Ste
Ec
Ca
Sta
Or
Rh
Si
High dT/dP
Intermediate dT/dP
Low dT/dP
T/P (°C/GPa)
1500
1000
500
Age (Ga)
0
1
2
3
4


Figure 6

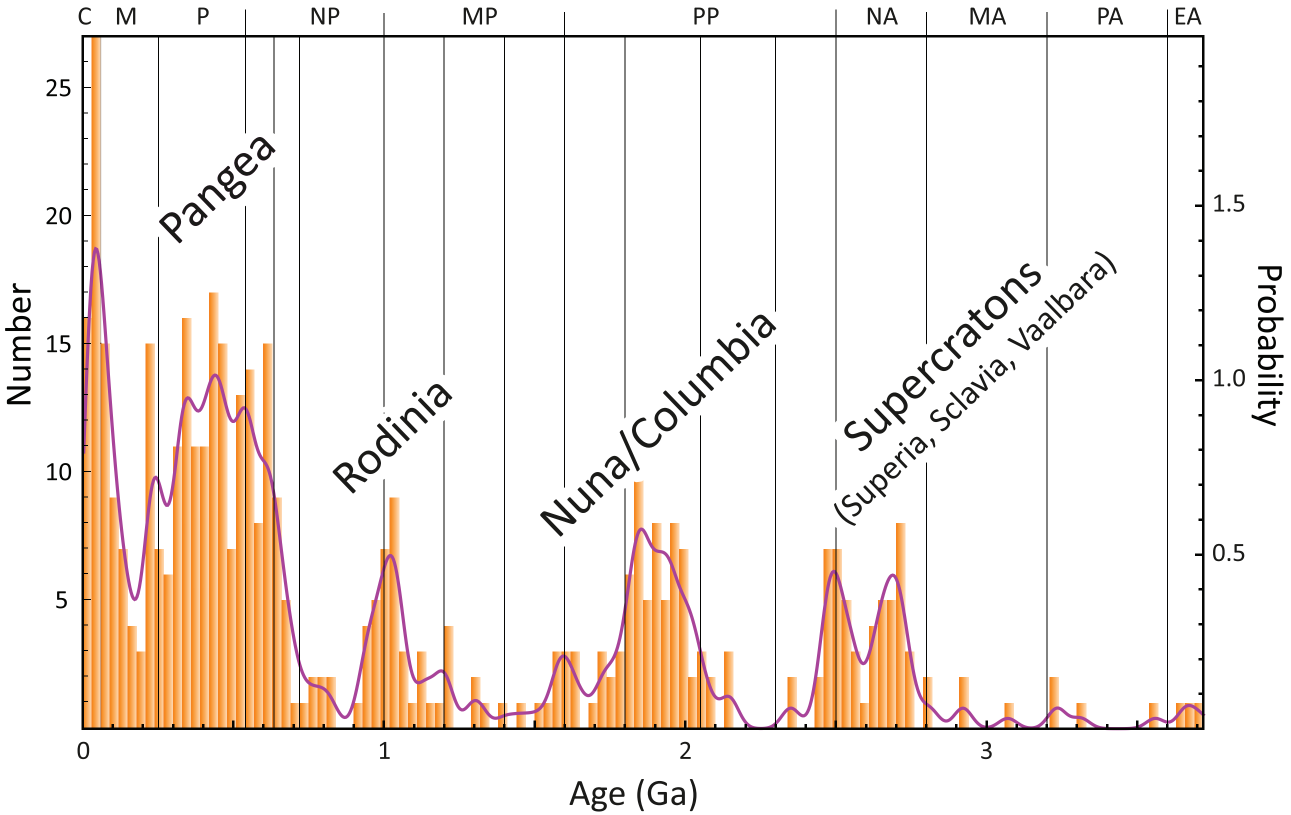
C
M
P
NP
MP
PP
NA
MA
PA
EA
Pangea
Rodinia
Nuna/Columbia
Supercratons
(Superia, Sclavia, Vaalbara)
Number
Probability
Age (Ga)
0
1
2
3
5
10
15
20
25
0.5
1.0
1.5

Figure 7

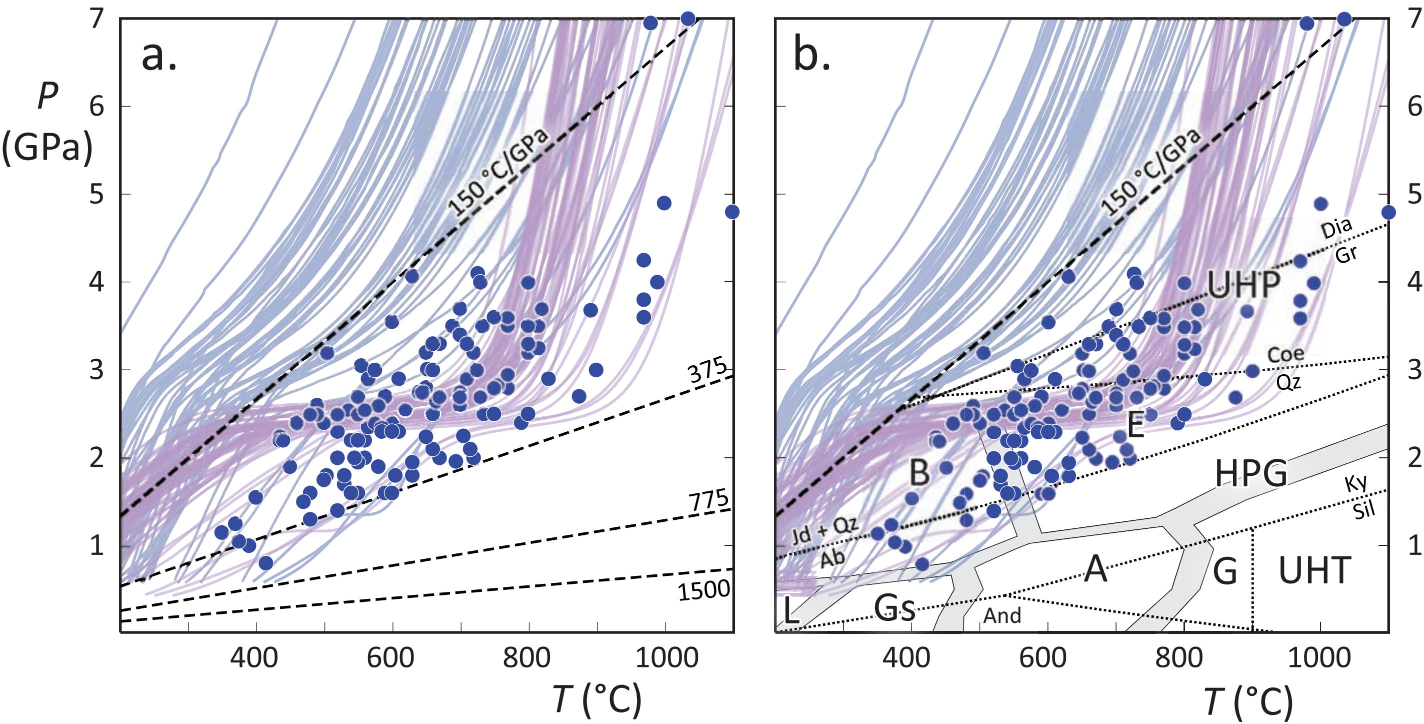

a.
b.
P (GPa)
T (°C)
150 °C/GPa
375
775
1500
Dia
Gr
UHP
Coe
Qz
E
HPG
Ky
Sil
B
Jd + Qz
Ab
A
G
UHT
L
Gs
And


Figure 8

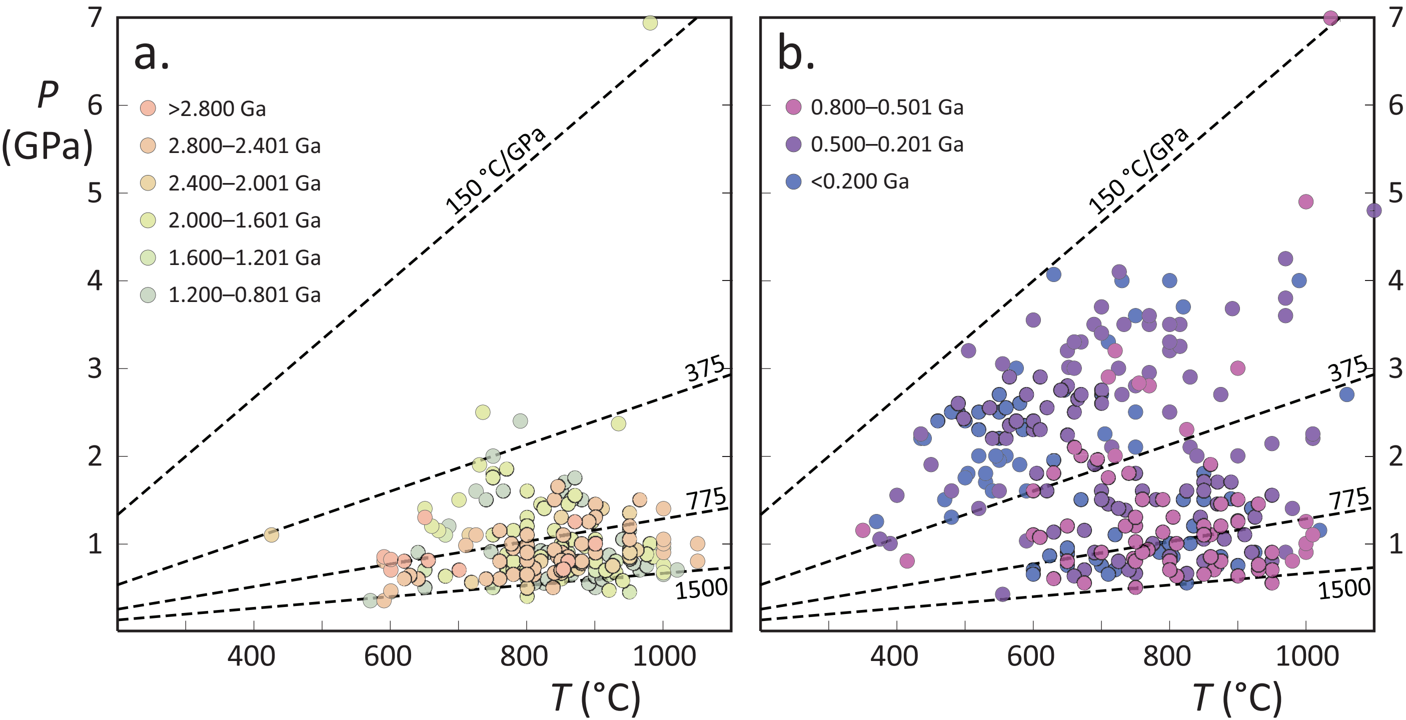

a.
b.
P (GPa)
>2.800 Ga
2.800–2.401 Ga
2.400–2.001 Ga
2.000–1.601 Ga
1.600–1.201 Ga
1.200–0.801 Ga
0.800–0.501 Ga
0.500–0.201 Ga
<0.200 Ga
150 °C/GPa
375
775
1500
T (°C)


Figure 9

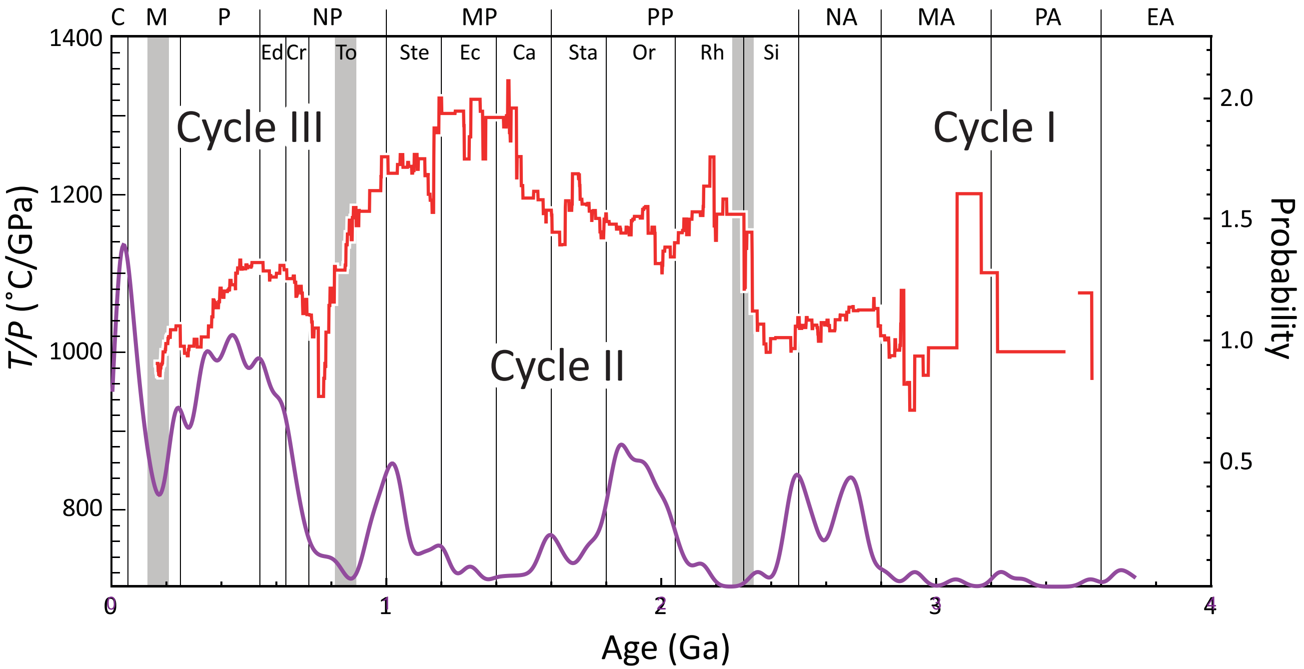

C
M
P
NP
MP
PP
NA
MA
PA
EA
Ed
Cr
To
Ste
Ec
Ca
Sta
Or
Rh
Si
Cycle III
Cycle II
Cycle I
T/P (°C/GPa)
Probability
Age (Ga)
1400
1200
1000
800
2.0
1.5
1.0
0.5
0
1
2
3
4


Figure 10